Volcanic sulfur emissions of Icelandic eruptions based on the petrological method

HÁSKÓLI ÍSLANDS

Veðurstofa Íslands

Volcanic sulfur emissions of Icelandic eruptions based on the petrological method

Eemu Ranta[1,2], Sæmundur A. Halldórsson[1], Bergrún A. Óladóttir[3], Melissa A. Pfeffer[3], Alberto Caracciolo[1], Enikő Bali[1], Guðmundur H. Guðfinnsson[1], Sara Barsotti[3], Sigrún Karlsdóttir[3]

[1]*Nordic Volcanological Center, Institute of Earth Sciences, University of Iceland, Iceland*
[2]*Now at Department of Geosciences and Geography, University of Helsinki, Finland*
[3]*Icelandic Meteorological Office, Iceland*

Cover: Gas and lava emitted from the main Fagradalsfjall vent. May 31st, 2021. © Eemu Ranta

Veðurstofa Íslands
Bústaðavegur 7–9
150 Reykjavík

+354 522 60 00
vedur@vedur.is

Skýrsla:

RH-08-23

Abstract

Outgassing of sulfur is one of the main local and global hazards posed by volcanic eruptions. Thus, advance information of the sulfur emission potentials of volcanoes is a key component of hazard assessments. Whereas direct measurement data are only available from recent Icelandic eruptions, the record of volcanic sulfur emissions can be extended back in time with indirect methods. Here, we use a petrological method based on the observation that the pre-eruptive sulfur contents of magmas—the main control on the magnitude of eruptive sulfur release—are conserved and can be measured in glassy silicate melt inclusions that were trapped within growing crystals at depth. This method has been applied previously to estimate sulfur emissions from several notable historical eruptions in Iceland (e.g., Laki 1783 CE), but estimates for most of Iceland's 33 volcanic systems have been missing. In this study, we extend this coverage by presenting total sulfur emissions potentials (ΔS_{max}, in units of kg S/kg melt) for 67 eruptions from 22 volcanic systems in Iceland based on a compilation of new and published melt inclusion and groundmass glass sulfur concentration data. These include new ΔS_{max} estimates for the 4 km^3 Fjallsendahraun 1382 CE fissure eruption and 14 eruptions from the latest volcanic episode (~700–1240 CE) in the Reykjanes Peninsula. The data show that sulfur emission potentials depend strongly on melt composition, and to a lesser degree on the volcanotectonic setting. In general, ΔS_{max} are moderate (~600–1300 ppm) in Mg-rich basaltic eruptions (>8 wt.% MgO) and low (0–400 ppm) in andesitic and rhyolitic melts (SiO_2 > 57 w%). A peak in ΔS_{max} values (700–2600 ppm, average ~1500 ppm) is seen in evolved basalts (4–8 wt.% MgO). Highest ΔS_{max} (~2100–2600 ppm) are found in three evolved basaltic eruptions in the South Iceland Volcanic Zone eruptions (Hekla 1913 CE, Eldgjá 939 CE and Surtsey 1963-67 CE). Our results can be used to assess volcanic gas hazards—for example as input data in gas dispersal models—at volcanoes where no direct measurements are available.

Útdráttur

Afgösun brennisteins er ein helsta umhverfisvá í nærumhverfi og á heimsvísu sem stafar af eldgosum. Því er mat á mögulegri brennisteinslosun eldfjalla einn af meginþáttum í hættumati. Þó beinar mælingar á brennisteinslosun séu eingöngu til frá nýlegum eldgosum á Íslandi þá er hægt að afla upplýsinga um losunina í fortíðinni með óbeinum aðferðum. Hér notum við bergfræðilega aðferð sem byggir á þeirri staðreynd að brennisteinsmagn í kviku fyrir gos, sem mestu ræður um umfang losunarinnar í gosi, varðveitist og er hægt að mæla í glerjuðum silikatbráðarinnlyksum sem lokuðust inni í vaxandi kristöllum niðri í jörðinni. Þessari aðferð hefur áður verið beitt til að meta brennisteinslosun í nokkrum af helstu sögulegum eldgosum á Íslandi (t.d. í Skaftáreldum árið 1783), en mat fyrir flest af 33 eldstöðvakerfum landsins skortir. Með þessari rannsókn aukum við við þekkinguna með því kynna heildar brennsteinslosunargetu (ΔS_{max}, með einninguna kg S/kg bráð) 67 eldgosa í 22 eldstöðvakerfum á Íslandi og byggir á samantekt á nýjum og áður birtum gögnum um brennisteinsstyrk í bráðarinnlyksum og grunnmassagleri. Þar með talið er nýtt mat á ΔS_{max} fyrir Fjallsendahraun, sem er frá árinu 1382 og 4 km^3 að rúmmáli, og 14 gos frá síðasta eldgosatímabili (~700–1240) á Reykjanesskaga. Gögnin sýna að brennisteinslosunargeta er mjög háð samsetningu bráðar og í minna mæli eðli jarðhniks í eldstöðvarkerfunum. Almennt eru ΔS_{max}-gildi miðlungshá (~600–1300 ppm) í Mg-ríkum basaltgosum (>8 % MgO af massa) og lág (0-400 ppm) í andesít- og rýólítbráð (SiO_2 > 57 % af massa). Toppur er í ΔS_{max}-gildum (700–2600 ppm, meðaltal ~1500 ppm) í þróuðu basalti (4–8 % MgO af massa). Hæstu ΔS_{max}-gildi (~2100–2600 ppm) finnast í þremur þróuðum basaltgosum í Suðurgosbeltinu (Hekla 1913, Eldgjá 939 and Surtsey 1963-67). Niðurstöður okkar má nota til mats á hættu af völdum eldgosagass, t.d. sem ílagsgögn fyrir gasdreifingarlíkön, frá eldfjöllum þar sem engar beinar mælingar hafa verið gerðar.

1 Introduction

Volcanic eruptions release vast quantities of volatiles (H_2O, CO_2, F, Cl and S) into the atmosphere. On geological timescales, volcanic outgassing regulates the composition of Earth's atmosphere (Gaillard et al. 2021). On short timescales, volcanic gases pose one of the principal hazards of eruptions. When gas plumes of large eruptions reach the stratosphere, volcanic sulfur (mainly released as SO_2) forms aerosols that block sunlight and cool the surface, with the potential to cause short-term hemispheric or even global climate perturbations (Robock 2000). In the troposphere, SO_2 reacts with water and oxidizes to form sulfuric acid and sulfate (SO_4^{-2}) aerosols, with both the gas and aerosol contributing to volcanic pollution that is one of the main environmental and health hazards for eruptions of all sizes (Schmidt et al. 2011, Oppenheimer et al. 2011, Gíslason et al. 2015, Carlsen et al. 2021, Stewart et al., 2021, Stefánsson et al. 2017). Assessing the sulfur release potential of future eruptions based on knowledge from past eruptions is a critical component of both long and short term hazard assessments.

Volatile concentrations in volcanic gas plumes can be measured by satellite instruments (e.g., Carn et al. 2017) or by ground-based measurements (e.g., Pfeffer et al. 2018). However, such direct measurements are only available for a relatively small selection of post-1970's eruptions globally (Oppenheimer et al. 2011).

Alternatively, volatile emissions from past eruptions can be constrained retroactively by indirect means. The 'petrological method' (Anderson 1974, Devine et al. 1984) utilizes the capacity of crystal-hosted silicate glass melt inclusions to retain high volatile concentrations, which in the right circumstances indicate the undegassed, pre-eruptive state of their host magmas (i.e., Lowenstern and Thompson 1995). The key advantage of the petrological method is that volatile emissions from any past eruption in the geological record where glassy melt inclusions are preserved can be calculated.

The petrological method has been previously applied for a selection of historical and recent Icelandic eruptions (Sigurdsson 1982, Óskarsson et al. 1984, Devine et al. 1984, Palais and Sigurdsson 1989, Métrich et al. 1991, Thordarson et al. 1996, 2001, 2003, Sigmarsson et al. 2013, Hartley et al. 2014, Haddadi et al. 2017, Bali et al. 2018). These studies reveal the massive atmospheric SO_2 loading resulting from large historical basaltic fissure eruptions in Iceland, exemplified by the Eldgjá 939 CE (~200 Mt SO_2; Palais and Sigurdsson 1989, Thordarson et al. 2001) and Laki 1783 CE fires (~120 Mt SO_2; Sigurdsson 1982, Óskarsson et al. 1984, Thordarson et al. 1996). However, the volatile emission potentials of most of the 33 active volcanoes in Iceland (www.icelandicvolcanos.is) are poorly constrained, leaving a large gap in our understanding of regional volatile systematics and limiting the ability to prepare for future volcanic degassing hazards.

Here, we present a database of melt inclusion and matrix glass volatile concentrations from 70 Icelandic eruptions, compiled from published data as well as new data from 7 eruptions. We use the database to review the volatile systematics of Icelandic volcanoes and to produce eruption-specific volatile emission estimates using the petrological method. We focus on sulfur, which is the most commonly measured volatile in melt inclusions, and provide S emission estimates for 67 eruptions. Our results, combined with total lava effusion measurements or estimates, can be used as input data for gas dispersal models (Barsotti 2020) and to thereby assess volcanic gas hazards prior to eruptions, most importantly when no direct measurements are available.

2 Geological setting

Iceland is an atypically volcanically active subaerial segment of the slow-spreading Mid-Atlantic Ridge, an ocean island hotspot located at the divergent plate boundary between North America and Eurasia (Fig. 1). Excess magmatism here is caused by interaction between the spreading center and a hot mantle upwelling, the Iceland mantle plume. At present, 33 volcanic systems in Iceland are considered active, with a collective average eruption interval of 4-5 years (Thordarson and Larsen 2007). The activity is concentrated in several rift segments, here divided into the Eastern, Northern and Western Rift Zones (ERZ, NRZ and WRZ) and the Reykjanes Peninsula (RP), the transform Mid-Iceland Belt (MIB), the propagating rift South Iceland Volcanic Zone (SIVZ) and two off-rift zones, Snæfellsnes Volcanic

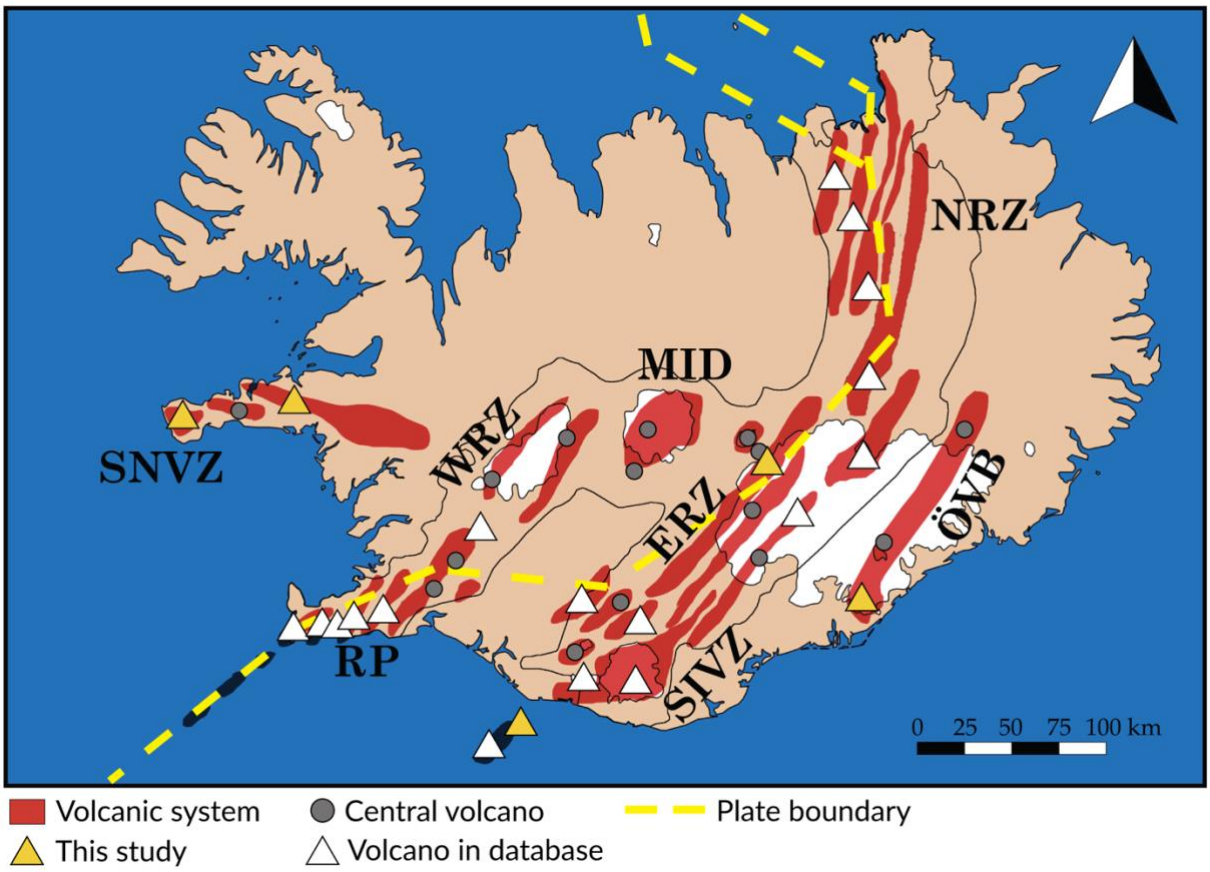

Figure 1. Map of Icelandic neovolcanic zones and volcanic systems. Volcanoes included in the Icelandic melt inclusion Catalogue and new data are indicated by white and yellow triangles, respectively.

Zone (SNVZ) and Öræfajökull Volcanic Belt (ÖVB) (Fig. 1). Eruption types vary from common effusive basaltic fissure eruptions (which may have explosive phases) to less frequent explosive silicic eruptions (Thordarson and Larsen 2007). Many volcanoes are located entirely or partly beneath glaciers; subglacial eruptions are often associated with a major explosive component. Silicic volcanics constitute up to 10% of the exposed bedrock (Jónasson 2007).

3 Methods and catalogue information

3.1 Samples and electron probe microanalysis

New major element and S and Cl concentration data for glassy melt inclusions (hosted in olivine, plagioclase and clinopyroxene) and matrix glasses are presented here from 7 eruptions from 5 volcanoes: (1) Fjallsendahraun (~1382 CE; also known as Frambruni), belonging to the Bárðarbunga volcanic system (Sigmarsson and Halldórsson 2015), is one of the largest Holocene fissure eruptions in Iceland. It is a tholeiitic lava flow with an estimated volume of ~4 km^3 (Thordarson and Larsen 2007). Two scoria samples were collected from two different craters from the eruptive fissure. (2) An unnamed Holocene trachybasalt lava at Djúpalónssandur in the SNVZ from the Snæfellsjökull volcano. The sample is scoriaceous lava crust. (3) Trachybasalt/basaltic trachyandesite Eldfell eruption that started January 23 1973 in the island of Heimaey in the SIVZ (Furman et al. 1991). Two tephra samples were used; ELD-2 is from the first day of eruption (January 23) and ELD-1 was collected from a 'vagabond' crater (collapsed piece of a crater that was transported by a lava flow) formed during a later stage of the eruption. (4) A scoria sample (BFR-1) was collected from one of the craters of the basaltic Grábrókarhraun lava near the village of Bifröst, which is the easternmost Holocene eruption of the SNVZ and thought to originate from the Ljósufjöll volcanic system. (5) Two basaltic (ÖRA-1 and ÖRA-3) and one basaltic

trachyandesite lava (ÖRA-2) of unknown age from Öræfajökull were collected from separate stratigraphic units by the Svínafellsjökull glacier. The lavas have a thick (> 1 cm) glassy crust and likely erupted subglacially.

Major element, S and Cl analyses were performed on hand-picked glasses and crystals by electron probe microanalysis (EPMA) with the JEOL JXA-8230 SuperProbe at the Institute of Earth Sciences, University of Iceland, which is equipped with five wavelength-dispersive spectrometers. The analytical settings were identical to those described in Caracciolo et al. (2020) and Ranta et al. (2022). Accuracy of the EPMA measurements and instrumental drift was monitored by analyzing the basaltic glass standard VG-A99 and the Lipari obsidian at the beginning and end of each session. The VG-A99 values for S (137±27 ppm) and Cl (196±22 ppm) (both 1σ, n = 12) agree within mutual uncertainty at 1σ level with published values (Supplementary Table 7).

3.2 Catalogue assemblage

The Iceland Melt Inclusion Catalogue (IMIC; Supplementary Table 1) was compiled from published geochemical melt inclusion (MI) data from Icelandic eruptions. The catalogue includes, to the authors' best knowledge, all published MI datasets to date (n = 36; references are listed in Table 1) that include measurements of one or more of the five major volatile elements in silicate melts: H (here given as H_2O), C (given as CO_2), F, S and Cl, or B. Where available, associated matrix glass analyses of the host lavas are also included in the database.

3.3 Coverage

IMIC contains a total of 4916 data points from ~70 individual eruptions. The data are categorized as melt inclusions (n = 2977), matrix glasses (n = 1819), subglacial glasses (n = 60) or embayments (n = 40). The data cover all volcanic zones of Iceland, namely the Eastern, Northern and Western Rift Zones (ERZ, NRZ and WRZ), the Reykjanes Peninsula (RP), the propagating rift South Iceland Volcanic Zone (SIVZ) and the two off-rift Snæfellsnes Volcanic Zone (SNVZ) and Öræfajökull Volcanic Belt (ÖVB) (Fig. 1). The individual volcanoes with most data points are Krafla (n = 956), Bárðarbunga (n = 820), Fagradalsfjall (n = 545) and Grímsvötn (n = 537) (Fig. 2). Compositionally, 84.78% of the analyses are basaltic (SiO_2 < 52 wt.%), 14.63% are silicic (SiO_2 > 65 wt.%), and 0.59% intermediate (SiO_2 = 52-65 wt.%). Of the volcanic zones, the SNVZ, ÖVB and WRZ have the poorest coverage with each constituting below 4% of the total, whereas the main active rift zones ERZ, NRZ and RP together contribute about 80% of the total.

3.4 Data type, quality and filtering

Volatile concentrations in volcanic glasses can be determined by microanalytical techniques which enable the analysis of melt inclusions as small as ~5 μm diameter. The most common analytical methods are secondary ion mass spectrometry (SIMS; H_2O, CO_2, F, S, Cl), electron probe microanalysis (EPMA; F, S, Cl), Fourier transform infrared spectroscopy (FTIR; H_2O, CO_2) and Raman spectroscopy (H_2O, CO_2). Data from all these methods are represented in IMIC. In order to retain the data integrity, no filtering was done, and published data are reported in IMIC as in the original publications. Volatile concentrations reported for MIs that have been rehomogenised under atmospheric pressure (Caracciolo et al. 2020, 2022) are considered unreliable due to possible volatile loss during reheating, and are not considered further.

Post-entrapment process (PEP) correction. Major and trace element and volatile concentrations in melt inclusions can be modified by post-entrapment crystallization and/or diffusive re-equilibration (e.g., Danyushevsky et al. 2000). PEP can significantly affect the concentrations of compatible elements in the residual melt (e.g., MgO; Fig. 3a) but is minor for most incompatible elements including volatiles (Fig. 3b). Some, but not all, studies perform PEP corrections to reconstruct original melt inclusion compositions. However, the correction schemes vary between studies and depend on the host-crystal. When possible, both the measured concentration data (i.e., prior to PEP corrections) as well as the reported PEP-corrected values are reported in IMIC. Thus, the catalogue user has access to unprocessed data and can opt to make PEP corrections using the method of choice.

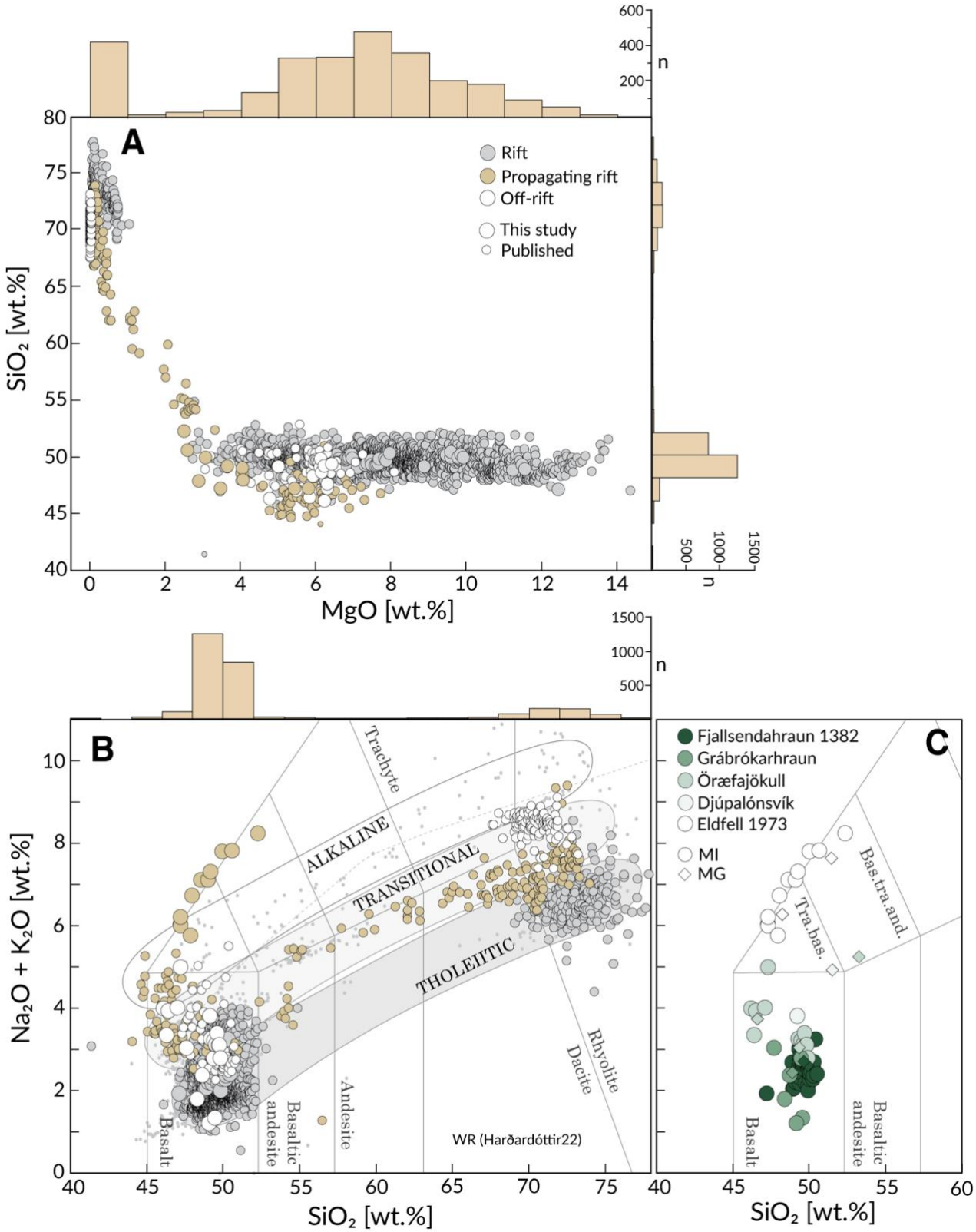

Figure 2. Overview of the Iceland melt inclusion catalogue (IMIC). **A** SiO_2 vs MgO. **B** Total alkali (Na_2O+K_2O) vs SiO_2 (TAS). The A and B panels show published melt inclusion data (matrix glasses, embayments and pillow glasses omitted). There is a broad overlap of melt inclusions with whole-rock data from Iceland from the compilation of Harðardóttir et al. (2022; grey dots in panel B). Histograms in **A** and **B** highlight that the data distribution is heavily skewed toward basaltic compositions. Only melt inclusion data from IMIC is shown. (c) A cropped TAS diagram with a detailed overview of new data.

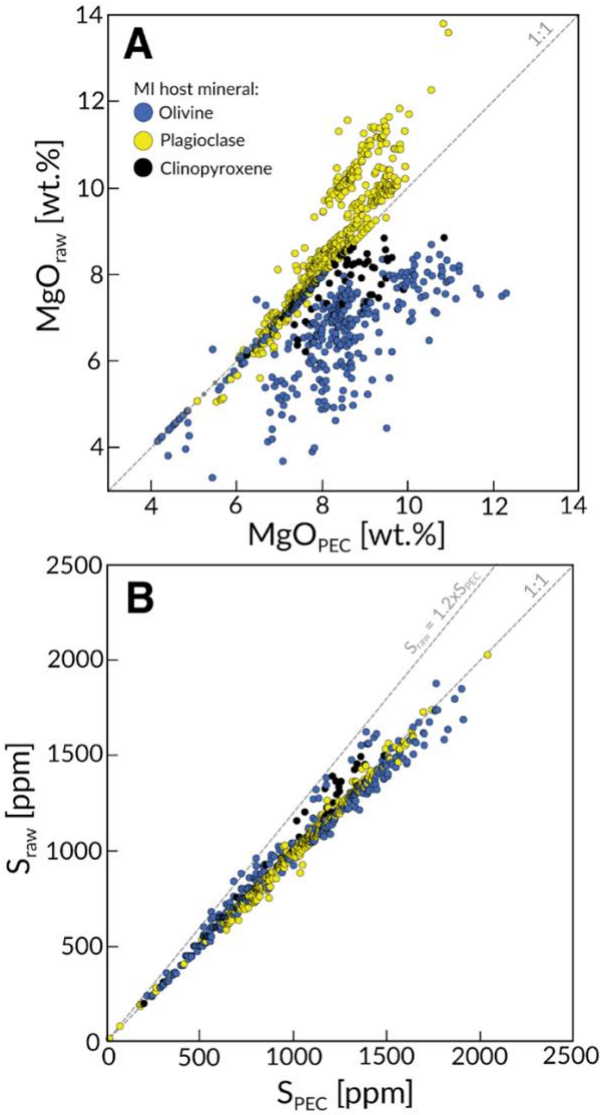

Figure 3. Effects of post-entrapment processes on (a) MgO, and (b) S concentrations of melt inclusions. Subscripts 'raw' and 'PEC' refer to uncorrected raw data and PEP-corrected data, respectively.

3.5 The petrological estimate of eruptive volatile emissions

3.5.1 Calculation of volatile fluxes based on the petrological estimate

If the pre-eruptive (C_0) and post-eruptive (C_1) volatile concentrations and the crystallinity (X_{cryst}) of a given eruption are known, the eruptive volatile release per unit mass of melt (ΔC, [kg volatile/kg melt]) can be calculated as

$$\Delta C = (1–X_{cryst})(C_0 – C_1) \quad (1)$$

Melt inclusions preserve high volatile concentrations that are used as an approximation of the pre-eruptive state (C_0) of a magma. In turn, matrix glasses—which most commonly either quenched rapidly after leaving the vent (tephra) or at the surface of a lava flow (lava crust)—provide an estimate of the post-eruptive volatile contents (C_1). Because the exact crystallinity of lavas is not reported for the majority of the eruptions in IMIC, we opt to use $X_{cryst} = 0$ for all ΔC calculations.

C_0 and C_1 are chosen differently depending on the volatile species. For H_2O, F and Cl, the average MI and matrix glass concentrations are used for C_0 and C_1, respectively. In cases where H_2O was not analyzed in matrix glasses it is assumed that $[H_2O]_1 = 0$, which is a reasonable assumption given the low H_2O concentrations in Icelandic bulk lavas and matrix glasses.

For sulfur, S_0 is chosen differently for melt compositions above and below MgO = 4 wt.% because of the pronounced effect of sulfide saturation on S concentrations in melts below that approximate threshold (Ranta et al. 2022; section 5.2). For melt compositions with MgO > 4 wt.%, S_0 is taken as the *highest* measured MI concentration (after discarding obvious outliers, always outside 75% confidence interval) following empirical evidence that this approach leads to close correspondence with observed emissions (Bali et al. 2018). For melts with MgO < 4 wt.% (low-MgO basalts to rhyolites), S_0 is chosen instead as the mean MI S content. For all melt compositions, S_1 is chosen as the *minimum* S concentration measured in matrix glasses. The minimum concentration is used due to an analytical bias toward higher concentrations than bulk erupted material, because analyses are generally performed on the fastest quenched glass (and hence least degassed) material.

Because S concentrations in tephra glasses from a single eruption may vary depending on how fast the sample was quenched (Sigmarsson et al. 2013, Liu et al. 2018), it is useful to differentiate between the apparent sulfur release at the vent

$$\Delta S_{vent} = S_0 – S_1 \quad (2)$$

and the maximum sulfur emission potential

$$\Delta S_{max} = S_0 \quad (3)$$

which reflects degassing of all pre-eruptive sulfur (i.e., $S_1 = 0$ in eq.2).

If the total dense rock estimate volume, V_{DRE} [m^3] (equivalent of vesicle-free solidified lava), and density, ρ [kg/m^3], of the erupted products are

known, the total mass of volatile release, m [kg], can be calculated as

$$m = \Delta C \times \rho \times V_{DRE} \quad (4)$$

The densities (ρ) of the solidified lava and the melt are assumed to be 2710 kg/m^3 for basalts, 2600 kg/m3 for intermediate rocks and 2470 kg/m^3 for silicic rocks (Sharma et al. 2008, Hartley and Maclennan 2019). For lavas with no reported V_{DRE}, we make the approximation

$$V_{DRE} = bV \quad (5)$$

where V is the estimated volume of tephra deposits or the lava flow volume and b is a scaling factor (between 0 and 1) that accounts for vesicularity. Commonly, V is calculated by

$$V = hA \quad (6)$$

where A [m^2] is the lava field area based on geological mapping and h [m] is the estimated average thickness of the lava. If the eruption duration t [s] is known, the average volatile emission rate R [kg/s] can be calculated as

$$R = m/t \quad (7)$$

Units. C and ΔC are given in parts per million by weight (ppm) for CO_2, F, Cl and S and weight percent (wt.%) for H_2O. Sulfur emissions are typically reported in the literature as kilo– or megatons, or teragrams of either S (total sulfur) or SO_2, which can be converted using 1000 kt = 1 Mt = 1 Tg = 10^9 kg, and $m_S = 0.5005 m_{SO2}$).

3.3 Caveats and sources of error of the petrological method

Several caveats need to be kept in mind when using the petrological method (Devine et al. 1984):

1. Melt inclusions do not always accurately record the volatile composition of the pre-eruptive melt. Volatile concentrations in MIs can strictly represent the pre-eruptive state of the melt *only if* they were trapped from the carrier melt shortly before eruption *and* were quenched rapidly enough to prevent diffusive modifications or post-entrapment crystallization. More commonly, MIs formed during an earlier stage of the magma's history. Then, decoupling of MI and host melt after entrapment partly shields the MI from subsequent magmatic processes (e.g., fractional crystallization, magma recharge, gas fluxing, vapor or sulfide saturation) that may have caused the host magma to either lose or gain volatiles. The common observation that MIs tend to be more primitive and chemically heterogeneous than carrier melts reflects such decoupling. This problem is partly overcome in our ΔS calculations by the choice of maximum MI S concentration, which is typically found in MIs with MgO contents that closely matches the carrier melt.
2. Different volatile species need to be treated separately because of their differing solubilities and diffusion rates in melts, and additional factors that affect their concentrations in melts and their preservation in melt inclusions:
3. Accurate CO_2 measurements in MIs are complicated by the necessity to account for vapor bubbles and mineral precipitates on the walls of the bubbles, which can host more than 90% of the CO_2 contained in the MI (Hartley et al. 2014, Moore et al. 2015, Rasmussen et al. 2020, Schiavi et al. 2020), and decrepitation, which leads to loss of CO_2 (Maclennan 2017). The CO_2 concentrations in vapor bubbles can be estimated by Raman spectroscopy and added to total MI CO_2 content. Raman measurements of vapor bubbles are included in IMIC if reported in the original publication.
4. Water, due to the high diffusivity of H^+, is especially prone to re-equilibration which can lead to both increased and decreased H_2O contents in the melt inclusion (Hauri et al. 2002, Gaetani et al. 2012, Barth and Plank 2021). On the other hand, this means that MIs are more likely to have equilibrated with their carrier melts with respect to H_2O, thus representing true pre-eruptive contents, although the same effect can cause post-eruptive re-equilibration with a degassed host melt.
5. The concentrations of F, Cl and S—all relatively slow-diffusing elements—are assumed to be only affected by post-entrapment crystallization, which leads to an increase of their concentrations in the residual melt. This distillation effect leads to only a small increase in the measured concentrations (< 5%) for the typically modest (< 15%) reported amounts of post-entrapment crystallization and is always less than 20% for published data (Fig. 2b).
6. Fluorine is present in anomalously high concentrations in some high-anorthite plagioclase-hosted melt inclusions in Iceland, which has been suggested to result by uphill

diffusion of F toward Al-rich grain-boundary melts during MI formation (Neave et al. 2014). Thus, F concentrations in plagioclase-hosted MIs should be treated with caution.

7. The petrological method only takes into account the volatile emission capacity of the erupted melt itself. Actual volcanic volatile emissions may additionally involve input from magmatic volatile phases or external sources of volatiles (see section 5.1.2). The petrological method also neglects post-eruptive outgassing from cooling lava, which is an additional source of volcanic pollution (Simmons et al. 2017, Sigmarsson et al. 2020). This effect disproportionately affects F and Cl, which only reach melt saturation as their concentrations in residual melts are driven up by microlite crystallization in cooling lava fields. Thus, petrological F and Cl emission estimates—often negligible (Fig. S2)—should be taken as minimum values.

4 Results

4.1 Overview of new data

The new EPMA data include major element compositions of matrix glasses (9 samples from 7 eruptions), melt inclusion glasses (n = 72) and their host crystals, i.e., olivine (n = 28), plagioclase (n = 47) and clinopyroxene (n = 3) (Supplementary Tables 3-6). The matrix glasses vary in composition from tholeiitic basalt (Fjallsendahraun 1382; MgO = 6.7 wt.%) to basaltic trachyandesite (Eldfell 1973; Fig. 2c). Of the two SNVZ samples, The Djúpalónsvík lava crust has an evolved trachybasaltic composition (MgO = 4.3 wt.%), whereas the Grábrókarhraun tephra glass and MIs are basaltic (MgO ≈ 6.0 wt.%) and less alkaline. Two of the Öræfajökull samples (ÖRA-1 and 3) are evolved basalts (MgO = 5.2 and 5.4 wt.%, respectively), and the third (ÖRA-2) is a basaltic trachyandesite (MgO = 2.75 wt.%) but lacks glassy MIs.

Notably, the Eldfell MIs lie outside of the compositional coverage of previously published MI data, being more alkaline and extending from trachybasaltic to basaltic trachyandesitic compositions (the latter exemplified by the ELD-2 tephra glass from January 23 1973, the first day of the eruption; Fig. 2c). These compositional trends echo the bulk rock compositions of the eruption (Furman et al. 1991).

Sulfur concentrations of Fjallsendahraun MIs can be divided into two groups: lower S contents from 860 to 1050 ppm are measured in a group of high-MgO (9.5–12.5 wt.%) melt inclusions hosted in high-An plagioclase ($An_{87.8–91.1}$), whereas higher S contents between 1200 and 1590 ppm (mean 1395±111 ppm, 1σ, n = 29, excluding a low-S outlier) are seen in remaining MIs which have lower MgO (7.1±0.6 wt.%, 1σ) and are hosted in plagioclase ($An_{81.3–89.3}$), olivine ($Fo_{78.8–84.9}$) and clinopyroxene ($Mg\#_{83.9–85.2}$). The Fjallsendahraun tephra is very similar in composition to other historic Bárðarbunga eruptions, also agreeing with previously reported compositions (Þórðardóttir 2020). The S contents of the high-S MIs are very similar to other published Bárðarbunga MI data (Bali et al. 2018, Caracciolo et al. 2020; Fig. 5).

4.2 Volatile concentrations of Icelandic melt inclusions

4.2.1. H_2O

Water contents of Icelandic melt inclusions vary from <0.1. wt.% in trace element-depleted rift basalts to up to 6.5 wt.% in silicic melt inclusions from Hekla. Overall, H_2O concentrations increase with increasing SiO_2 (Fig. 4a) and are lowest in basaltic MIs (0-1.5 wt.‰), moderate in intermediate MIs (0.7-4 wt.%) and highest, but also highly variable in silicic melts (0.1 to 6.5 wt.%). Among basalts, highest H_2O contents are seen in flank zone eruptions of Surtsey 1963-67 (1.2±0.1 wt.%, 1σ) and Fimmvörðuháls 2010 (0.9±0.1 wt.%) in the SIVZ and in the Berserkjahraun eruption of Ljósufjöll (0.7±0.3 wt.%) in SNVZ. Rift basalts tend to have lower MI H_2O contents, for example 0.36±0.14 wt.% in Holuhraun 2014-15, and 0.23±0.02 wt.% in Fagradalsfjall 2021. The lowest MI H_2O contents are observed in highly trace-element depleted, high-MgO (> 9 wt.%) basalts such as Miðfell (0.07±0.01 wt.%) in the WRZ and Heilagsdalsfjall of Fremrinámar in the NRZ (0.05±0.01 wt.%). Silicic MI H_2O contents from the Askja 1875 eruption vary from 0.6 to 2.7 wt.% (excluding outliers) with an average of 1.6±0.7 ‰. Compared to Askja, 2-3 times higher average MI H_2O contents are found in the silicic Hekla eruptions 1104 (3.1±1.2 wt.%), H3 (3.5±1.2 wt.%) and H4 (5.7±0.6 wt.%), and the rhyolitic Öræfajökull 1362 (3.1±0.6 wt.%) eruption. Of intermediate Hekla eruptions, the andesitic 1845 and the 1991 basaltic andesite eruptions have MI H_2O contents of 2.1± wt.% and 1.2±0.4 wt.%, respectively.

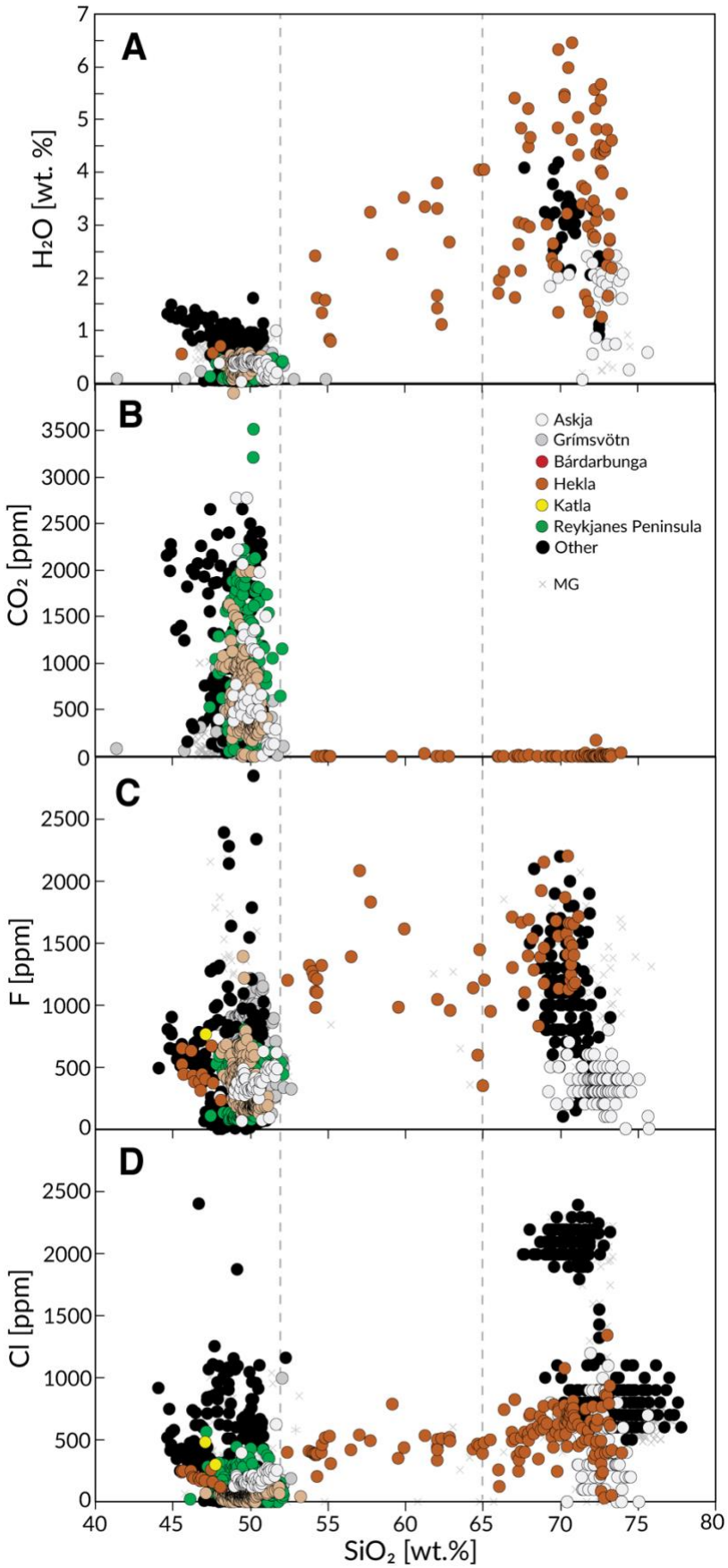

Figure 4. Effect of melt composition on volatile contents. SiO_2 plotted against (a) H_2O, (b) CO_2, (c) F and (d) Cl. Data from the Iceland Melt Inclusion Catalogue (IMIC; Supplementary Table 1)

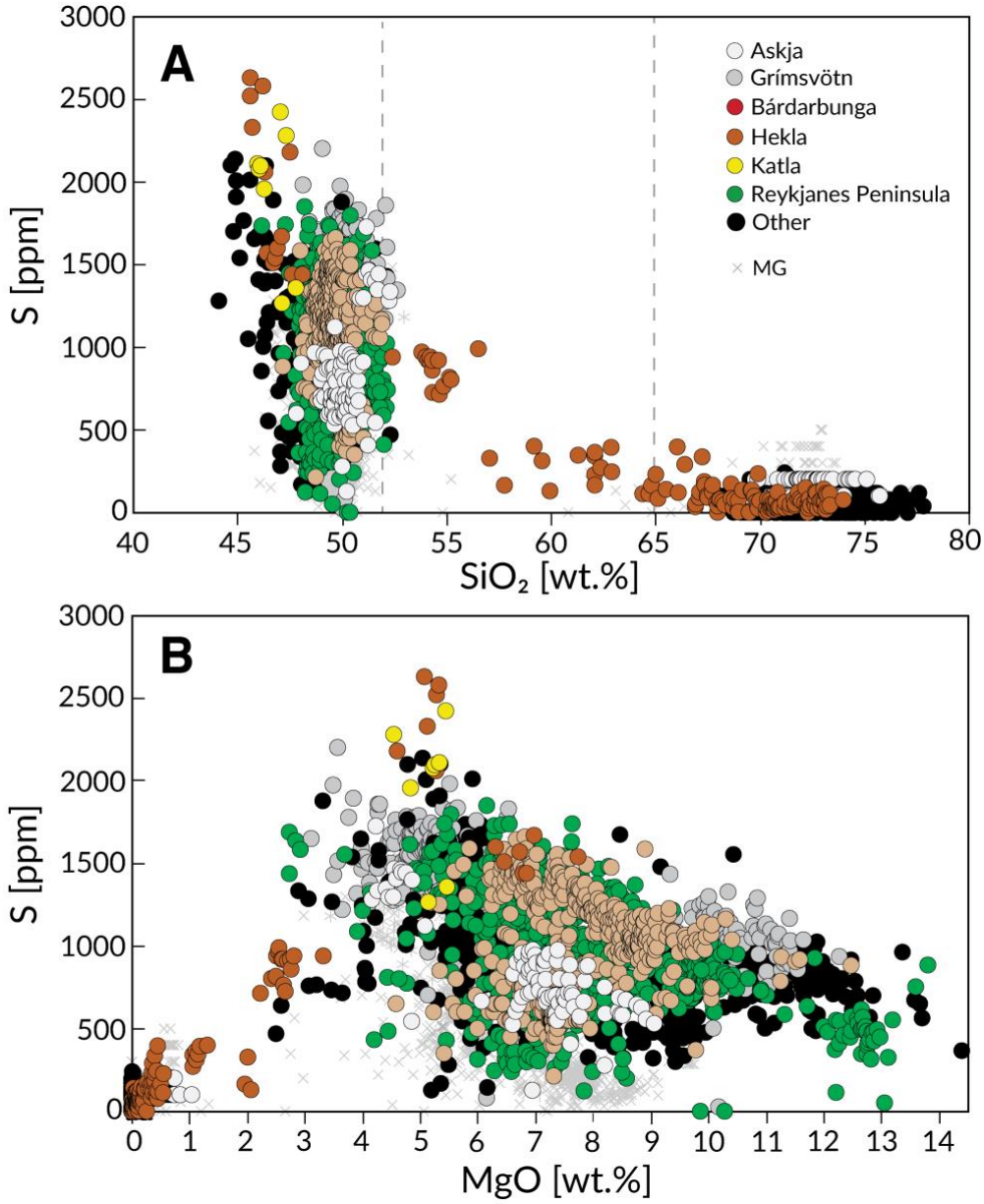

Figure 5: Compositional controls on sulfur contents of Icelandic melt inclusions. S vs. (a) SiO_2, and (b) MgO.

4.2.2 CO_2

The CO_2 concentrations in Icelandic MIs vary between 0 and 5960 ppm (Fig. 4b), but rarely exceed 3000 ppm. Only basaltic MIs show elevated CO_2 contents, whereas, as a rule, intermediate and silicic MIs have low CO_2 contents (< 50 ppm) that are indistinguishable from matrix glasses. It should be noted that in bubble-bearing melt inclusions, vapor bubbles may host close to 100% of the total MI CO_2 content, but only a few studies have measured and quantified the CO_2 content in the bubbles (Hartley et al. 2014, Neave et al. 2014, Bali et al. 2018). Thus, apparent CO_2 systematics are likely to be affected by sporadic underestimation of true MI CO_2 contents.

4.2.2 Fluorine

Fluorine contents of basaltic MIs range from < 50 ppm in primitive (> 10 wt.% MgO) rift zone basalts to 2850 ppm in the SNVZ Berserkjahraun eruption (Fig. 4c). Apart from Berserkjahraun, all F concentrations in basaltic MIs are below 1000 ppm. Intermediate MIs have between 980-2090 ppm F. Silicic MIs have highly variable F contents from 100 to 2200 ppm. The silicic Askja 1875 MIs lack the high F contents present in the silicic eruptions of Hekla and Öræfajökull with a range of 200-600 ppm. On average, there is no significant difference between matrix glass and MIs in either average F contents or variability. Fluorine concentrations in plagioclase-hosted MIs are not considered here and

are excluded from Figure 3, as they commonly show anomalously high concentrations that reflect the crystallization process rather than the pre-eruptive melt (Neave et al. 2017).

4.2.2 Chlorine

Basaltic MI Cl concentrations vary between 3 and 1900 ppm (Fig. 4d), excluding a single Fimmvörðuháls MI with 2500 ppm. Intermediate MIs (only available from Hekla) have a rather limited Cl range of 210-790 ppm. Silicic MIs have the highest, but most variable Cl contents of 0-2400 ppm.

4.2.2 Sulfur

Sulfur concentrations in MIs vary between 3 and 2630 ppm (Fig. 5). The S concentrations are highest in basaltic MIs, with a mean of 1010±380 ppm, decreasing with increasing SiO_2 to 650±300 ppm in intermediate to 80±60 ppm in silicic MIs (Fig. 5a). Most variability is seen basaltic MIs, where S is lower (~300-1300 ppm) in primitive high-MgO (> 10 wt.%) basalts and increases with decreasing MgO toward peak S contents (~1000-2630 ppm) at about 5 wt.% MgO (Fig. 5b). At the low-MgO side of this inflexion point, S contents steadily decrease toward intermediate and silicic rocks, which have 0-240 ppm S.

5 Discussion

5.1 Controls on volatile concentrations of Icelandic magmas

5.1.1 Mantle source, partial melting and regional variability

The volatile contents of primary basaltic melts are essentially controlled by the volatile content and the extent of melting of their mantle source. A number of studies have shown that the mantle beneath Iceland is heterogeneous with respect to the volatile origin (and probably, volatile concentrations) on a regional scale (e.g. Poreda et al. 1986, Hilton et al. 2000, Nichols et al. 2002, Füri et al. 2010, Halldórsson et al. 2016a, 2016b, Miller et al. 2019, Matthews et al. 2021, Marshall et al. 2022, Ranta et al. 2022). Given this, and that the degree of mantle melting is largely controlled by the tectonic setting—melting degree being high near the rift zones, and lower in the off-rift zones (Harðardóttir et al. 2022)—regional variations would be expected to be expressed in the volatile concentrations of MIs. For example, 2% partial melting of a mantle with 200 ppm H_2O (assumed to be perfectly incompatible) will yield a primary basaltic melt with 1 wt.% H_2O, whereas 20% partial melting would yield a melt with 0.1 wt.% H_2O—a factor of 10 less (assuming accumulated fractional melting). On the other hand, if mantle component A has 200 ppm H_2O and mantle component B 1000 ppm H_2O, equal degrees of melting will lead to a 5x difference in the H_2O contents of their respective primary melts. Such differences are well within the suggested variability in both melt degrees across different volcanic regions of Iceland (e.g. Koornneef et al. 2012) and the range of volatile concentrations inferred for the enriched and depleted mantle sources of mid-ocean ridge basalts (MORBs; Shimizu et al. 2016).

Such regional controls appear to influence H_2O and Cl, and to a lesser extent F concentrations of Icelandic basalts. Highest H_2O (up to 1.6 wt.% at Ljósufjöll and 1.5% in Surtsey), Cl (up to 2410 ppm at Fimmvörðuháls, 1880 ppm in Snæfellsjökull, 1260 ppm at Ljósufjöll) and F (2850 ppm, Ljósufjöll) concentrations are all seen seen in MIs of off-rift basalts in the SIVZ and SNVZ, whereas rift basalts (NRZ, ERZ, WRZ, RP) typically have lower H_2O (< 0.8 wt.%), Cl (< 500 ppm) and F (< 800 ppm) concentrations (Figs. 4 and 6). The Cl concentrations in basaltic MIs correlate with indicators of degree of melting, such as the ratio La/Sm (Fig. 6a, R^2 = 0.64), which increases with decreasing melt degree.

However, regional systematics do not appear to govern magmatic S contents (Figs. 5 and 6b). Instead, S contents of MIs from both rift and off-rift regions are similar at similar MgO or SiO_2 contents (Fig. 5), and do not correlate with La/Sm (Fig. 6b; R^2 = 0.07). Thus, melt S concentrations cannot be solely affected by melt degree and must be governed by another process.

Additional information is provided by the MI S/Cl ratio—which should stay approximately constant during partial melting and fractional crystallization due to the similarly incompatible nature of both elements. Off-rift MIs have low S/Cl ratios between 0.5 and 5, lower than either the depleted (S/Cl ≈ 250) or enriched (S/Cl ≈ 7.5) mantle endmembers inferred for the MORB source mantle (Shimizu et al. 2016; Fig. 6c). By contrast, highly depleted MIs in rift basalts (products of high-degree melting) have high S/Cl ratios (>100) approaching the S/Cl signature of the depleted

mantle (Fig. 6c). The decoupling of S systematics from Cl suggests that S concentrations in primary melts are buffered by sulfide saturation during mantle melting (Momme et al. 2003, Ding and Dasgupta 2018). Low-degree mantle melting that produces off-rift magmas may be more likely to occur under sulfide-saturated conditions. At high melt-degrees, sulfides originally present in the mantle source may be exhausted completely. This would lead to sulfide-undersaturated melting conditions after which S would behave as an incompatible element, producing melts with increasingly high S/Cl ratios.

5.1.2 Crustal magma evolution

Fractional crystallization during magma evolution leads to increasing concentrations of dissolved volatiles, which tend to behave as incompatible elements in the melt, *but only* until volatile-bearing fluid or solid phases are saturated. As vapor saturation, sulfide saturation and apatite formation are common during crustal magma evolution, volatile concentrations in MIs do not generally form simple correlations with SiO_2 (Fig. 4) or MgO (Fig. 5b).

Vapor saturation. Volatile solubility in basaltic melts in the upper crust usually increases in the order $CO_2 < S < H_2O < Cl \approx F$. Because of the low solubility of CO_2 at crustal pressures and inferred high CO_2 contents of primary melts, virtually all Icelandic basalts saturate a CO_2-rich vapor phase already at great depth, with only a few possible exceptions (e.g. Hauri et al. 2018, Miller et al. 2019, Matthews et al. 2021). As a result, the highest CO_2 contents are typically found in primitive MIs, but are negligible in intermediate and silicic rocks (Fig. 4b). At the other end of the solubility spectrum, H_2O, Cl and F remain undersaturated in basaltic melts at typical storage pressures, leading to increasing concentrations with decreasing MgO observed in basaltic pillow rim glasses (Nichols et al. 2002, Halldórsson et al. 2016b) and MIs.

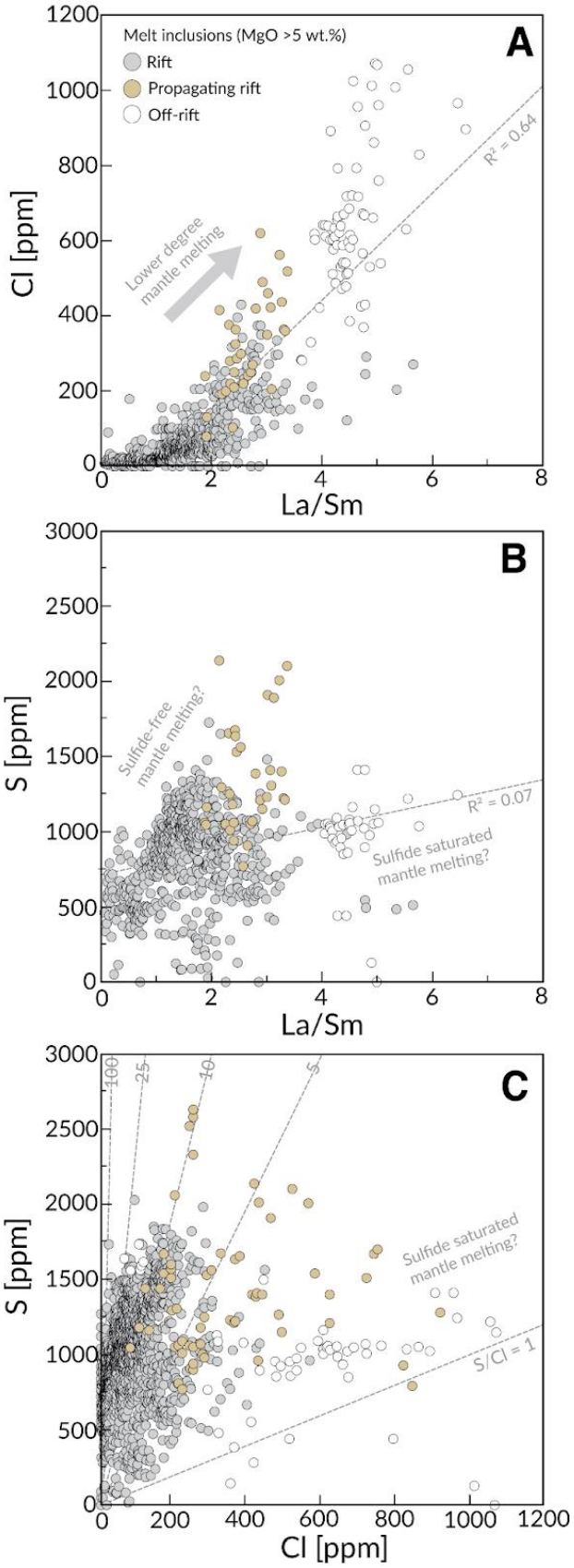

Figure 6. Effect of mantle melting and source heterogeneity on Cl and S systematics.

For silicic rocks, the H_2O-F-Cl systematics are more complicated. Silicic MIs of single eruptions can have highly variable H_2O-F-Cl contents, likely due to the daisy-chained effects of a complicated magmatic history involving fluid exsolution, brine assimilation, recharge, gas fluxing and crustal assimilation that may occur in silicic magma mushes in Iceland that may have lifetimes of 100s of thousands of years (Gunnarsson et al. 1998, Schattel et al. 2014, Padilla et al. 2016, Ranta et al. 2021). These effects are limited at off-rift settings, where silicic magma genesis may approximate closed system fractional crystallization paths (Martin and Sigmarsson 2007, Schattel et al. 2014), resulting in higher concentrations and smaller variability of H_2O and, F and Cl. Opposing behavior is sometimes observed between H_2O and the halogens; for example, silicic Hekla MIs have highest H_2O concentrations in Iceland, but are the most Cl poor (Fig. 4a,c; Ranta et al. 2021).

Sulfur has an intermediate solubility in basaltic melts and remains largely dissolved at crustal magma storage pressures. Instead, pre-eruptive sulfur concentrations and hence, eruptible sulfur content, ΔS, of Icelandic magmas—where sulfur is mainly dissolved as S^{2-}—are principally controlled by sulfide saturation, which leads to S sequestration by an immiscible sulfide melt (Fig. 7, Ranta et al. 2022). Moderate S (and ΔS) in primitive basalts (MgO > 8 wt.%) increase due to fractional crystallization to a peak in evolved basalts (MgO = 4-6 wt.%; Fig. 8a). At this point, melt sulfur concentrations reach the sulfur carrying capacity of melts (SCSS; sulfur concentration at sulfide solubility). Subsequent melt evolution leads to systematically decreasing S and ΔS due to immiscible sulfide melt formation and decreasing sulfide solubility, which rapidly decreases as FeO decreases (O'Neill and Mavrogenes 2002, Liu et al. 2007; Fig. 7). Consequently, moderate S concentrations and ΔS are observed in basaltic andesites, and lowest S and ΔS values are systematically found in dacites and rhyolites (Fig. 9a). In addition to melt composition, sulfur solubility further depends on various other parameters, with pressure, temperature, oxygen fugacity and sulfide composition being the most important (e.g., Smythe et al. 2017).

Error!

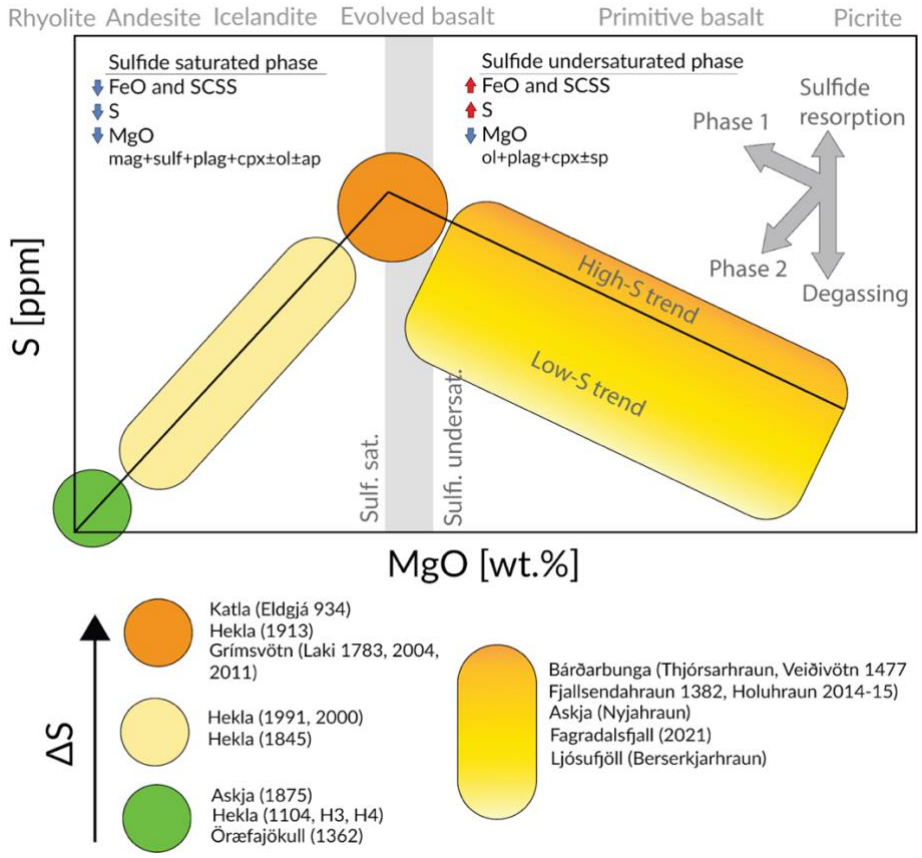

Figure 7. Petrological controls on S emission potential. SCSS = sulfur concentration at sulfide saturation. Phase 2 depicts a sulfide saturated phase, where the SCSS is decreasing due to removal of FeO from the melts.

Crustal assimilation potentially influences the H_2O-F-Cl contents of silicic rocks in Iceland (Schattel et al. 2014, Ranta et al. 2021), but is not likely to add S to the melt due to the S-poor nature of the dominantly igneous Icelandic crust (Torssander 1989).

5.2 Magmatic volatile phases and excess degassing

An inherent assumption of the petrological method is that volatiles that degas during an eruption are solely derived from the volume of the erupted lava. This assumption does not account for volatiles that may coexist with magmas in a separate magmatic volatile phase (MVP), which may be an accumulative product of a larger volume of magma that has reached volatile saturation in the magma storage region (Shinohara 2008, Edmonds and Wood 2018). Thus, the petrological estimate (only accounting for the dissolved volatiles) may underestimate the total volatile emissions (dissolved volatiles + MVP). One of the main factors controlling the volatile saturation state of a magma and thereby, the development of a MVP, is the pre-eruptive magma storage pressure (i.e., depth).

In basalts, because of the low solubility of CO_2 leading to loss of CO_2 during early stages of melt evolution, and the erratic preservation potential of CO_2 in MIs (Matthews et al. 2021), petrological estimates for eruptive CO_2 emissions should be considered inaccurate.

Underaccounting of S emissions by the petrological method has been repeatedly observed at arc volcanoes, something known as the 'excess degassing problem' (e.g. Andres et al. 1991, Sharma et al. 2004, Shinohara 2008, Su et al. 2016). A modified petrological method was thus proposed by Scaillet and Pichavant (2003) and Scaillet et al. (2003), that accounts for the existence of a MVP by assuming 1-5 wt.% of free gas phase at depth, that is added to the petrological estimate. However, the amount of MVP in basaltic Icelandic magma reservoirs is likely to be significantly lower due to the low H_2O concentrations (0.05-1 wt.%) of Icelandic basalts (Nichols et al. 2002) relative to arc magmas (> 2 wt.%, Plank et al. 2013). At typical Icelandic magma reservoirs pressures of 1–6 kbar (Neave et al. 2019), virtually all S, H_2O, Cl and F in low-H2O basaltic melts remain dissolved in the melt at their observed concentration ranges (e.g., Wallace and Edmonds 2011). This implies that the petrological method is suitable for recording Icelandic S emissions.

5.3 Empirical verification of the petrological estimate of SO_2 emissions

A critical accuracy test of the petrological method is to compare estimated SO_2 emissions with direct volcanic gas measurements.

5.3.1 Fissure eruptions

The best available test cases in Iceland are the recent Holuhraun 2014-15 (Bali et al. 2018, Pfeffer et al. 2018) and Fagradalsfjall 2021 (Pedersen et al. 2021, Halldórsson et al. 2022) basaltic fissure eruptions, that both lasted about 6 months. For both eruptions, lava effusion rates, lava volumes and gas fluxes are well constrained by ground-based measurements. The average lava effusion rate (90 m^3/s) and total lava volume (1.44 km^3 incl. vesicles) of Holuhraun (Pedersen et al. 2017) were approximately 10-fold compared to the 9.5 m^3/s and 0.15 km^3, respectively, measured for Fagradalsfjall (Pedersen et al. 2021). In both cases, the total SO_2 emissions derived from petrological estimates and gas measurements match remarkably well; the petrological estimate of 10.5 Mt SO_2 for Holuhraun (Bali et al. 2018) compares well with the 9.6 (6.7-14.3) Mt SO_2 (Pfeffer et al. 2018) derived from direct plume measurements by differential optical absorption spectroscopy (DOAS).

Petrological estimates of SO_2 have also been shown to agree reasonably well with satellite-based measurements using the Total Ozone Mapping Instrument (TOMS; Sharma et al. 2004) for the Krafla 1984 (0.64±0.19 vs. 0.4+0.04–0.15 Mt) Mt and Hekla 2000 (0.48±0.14 vs. 0.10±0.05 Mt) eruptions (Sharma et al. 2004). By contrast, similar comparisons at arc volcanoes sometimes show orders of magnitude higher TOMS SO_2 emissions relative to petrological estimates (Sharma et al. 2004). The close match between direct SO_2 measurements with the petrological method for hitherto observed Icelandic fissure eruptions provides an empirical validification of the petrological method as an accurate means to estimate volcanic SO_2 emissions of basaltic fissure eruptions in Iceland.

5.3.2 Explosive eruptions

Comparable direct and petrological SO_2 emission estimates are available for two Icelandic explosive eruptions (i.e., where degassing was dominated by high-altitude plumes):

Hekla 1980 (Sharma et al. 2004) and Grímsvötn 2011 (Sigmarsson et al. 2013). The two methods match reasonably well for the Hekla 1980 eruption (0.36±0.12 Mt SO_2 vs. 0.50±0.10 Mt SO_2 via TOMS). However, the estimated S emissions for the Grímsvötn 2011 eruption are about five times lower using the NASA satellite-borne Ozone Monitoring Instrument (OMI) (0.2 Mt S, or c. 0.3 Mt including estimated S scavenging on tephra surfaces; Olsson et al. 2013) relative to the petrological method (1.47±0.36 Mt, Sigmarsson et al. 2011, Haddadi et al. 2017).

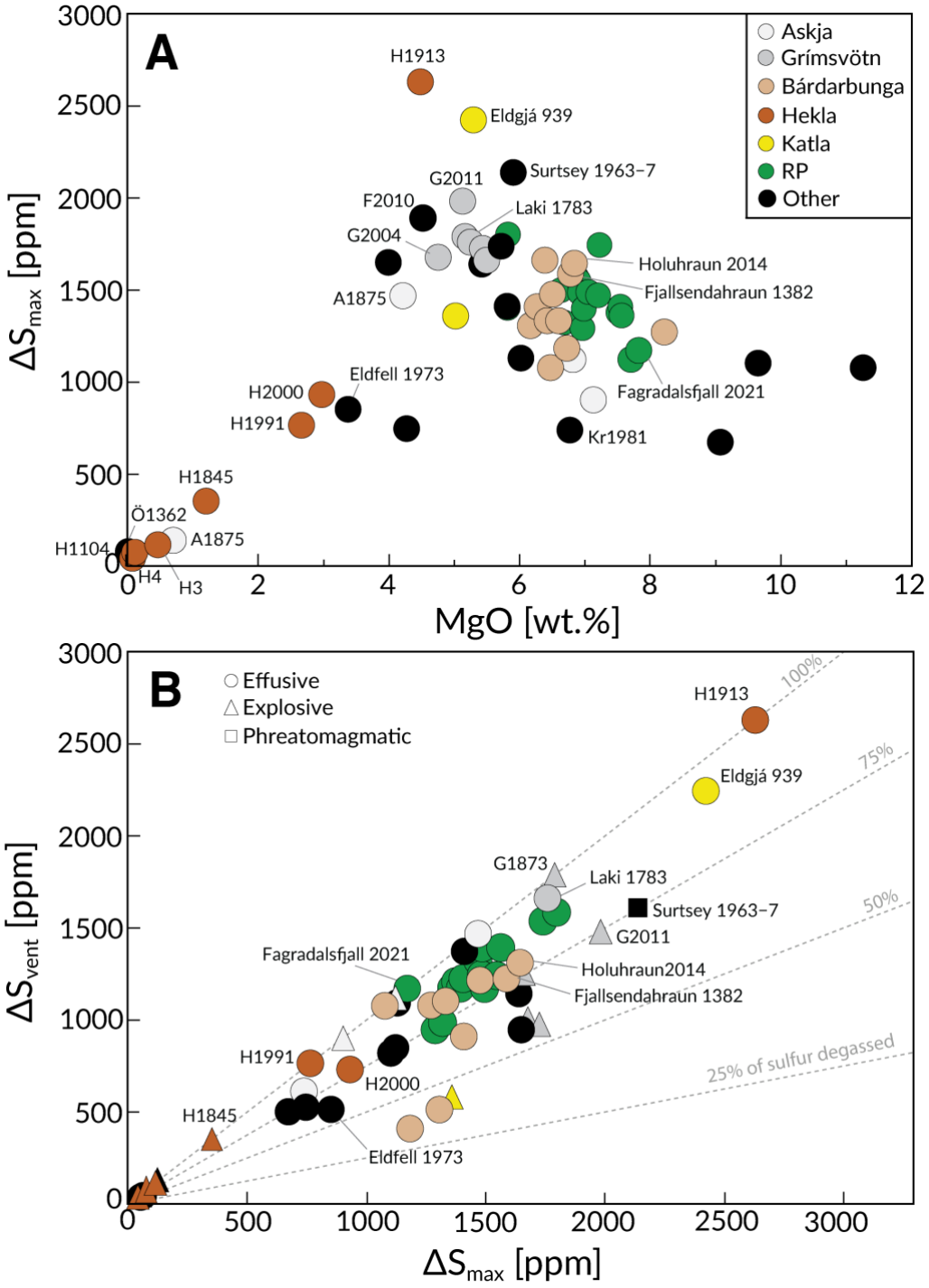

Figure 8: Petrological S emission estimates (a) ΔS_{max} vs. MgO, (b) Total sulfur emission potential ΔS_{max} compared to vent sulfur emissions (ΔS_{vent}). There is no obvious correlation between eruption type (explosive, effusive, phreatomagmatic) and ΔS. Plotted major element compositions of eruptions in Figs. 8a and 9a are based on average matrix glass compositions (Table S2).

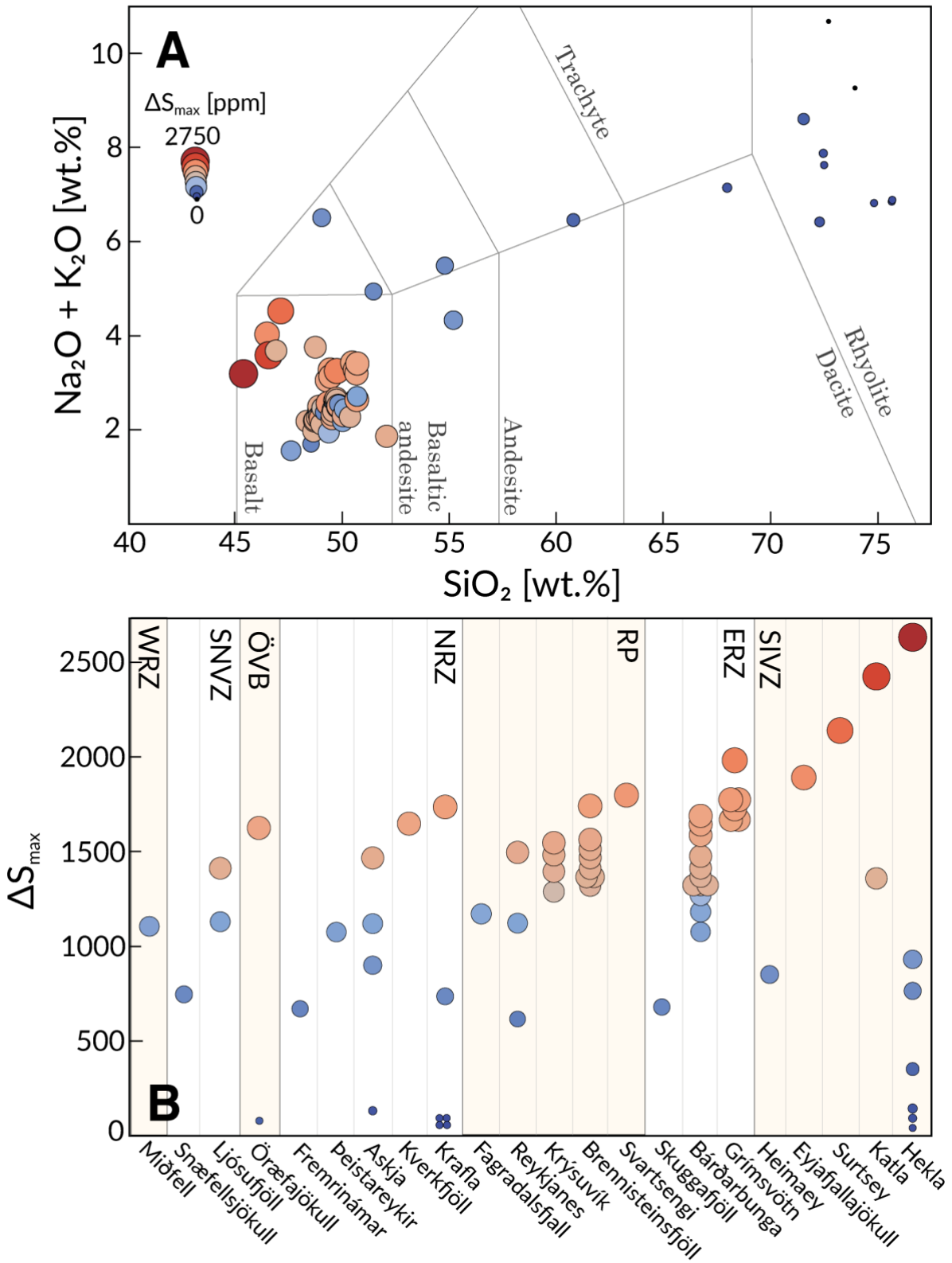

Figure 9. Summary figure of the sulfur emission potentials (ΔS_{max}) of Icelandic volcanoes. (a) TAS diagram. Circles represent individual eruptions and are shaded from blue to red, and increase in size, with increasing ΔS_{max}. (b) ΔS_{ma} sorted by volcano. Volcanoes are grouped by volcanic zone and increasing ΔS_{ma}

5.4 Sulfur emissions of Icelandic eruptions

The sulfur emission potentials (ΔS_{max}, ΔS_{vent}) for 62 Icelandic eruptions, calculated with the petrological method, are summarized in Table 2 and Figs. 8-9. An extensive summary including calculation details is available in Supplementary Table 2.

5.4.1 Largest S emitters in Iceland

The largest pre-eruptive sulfur concentrations in Iceland (ΔS_{max} > 1200 ppm) are systematically found in evolved basalts (MgO between 4 and 8 wt.%; Fig. 8a) irrespective of volcanic zone (Fig. 9b). This is also the most common compositional range of Icelandic eruptions (Fig. 2a), including the most frequently erupting Holocene volcanoes Grímsvötn, Bárðarbunga and Katla and the largest Holocene eruptions by volume (Þjórsárhraun, Laki 1783, Eldgjá 939). Basaltic eruptions at the higher end of this range (6-8 wt.% MgO), characterizing, e.g., Bárðarbunga and RP eruptions, have somewhat lower ΔS_{max} relative to the more evolved (4–6 wt.% MgO) eruptions typical of Katla and Grímsvötn (Fig. 8a).

Exceptionally high sulfur emission potentials (ΔS_{max} > 1800 ppm) are seen in five eruptions, all within a narrow range in MgO between 4.5 and 6 wt.% (Fig. 8a). This coincides with the apparent sulfide solubility peak in Icelandic melts (Fig 7, Ranta et al. 2022). Four of these eruptions, Eldgjá 939, Hekla 1913, Surtsey 1963-7 and Fimmvörðuháls 2010, are located in the SIVZ and have a mildly alkaline composition (SiO_2 < 48 wt.%, TAS > 3 wt.%; Fig 9). Thus, up to 50% higher S emissions may be expected for basaltic eruptions in the SIVZ relative to average basaltic rift zone eruptions.

Compared to arc volcanoes, Icelandic eruptions tend to have higher ΔS (Fig. 10), and thus emit more sulfur per unit mass of erupted material. This is largely a function of the dominant eruption composition in Iceland (relatively evolved basalts) coinciding with a maximum in dissolved S contents. By contrast, although basaltic arc magmas can have even higher S contents (several thousands of ppm) due to their generally more oxidized nature (Wallace and Edmonds 2011), basaltic arc eruptions are relatively uncommon.

5.6 Knowledge gaps and suggestions for future research

Data gaps to fill. Some large gaps remain in the regional coverage of available volatile MI data from Iceland. Of the large active volcanic systems in Iceland, there is a notable lack of data from Langjökull and Hofsjökull. Katla, one of the most productive volcanoes during the Holocene (Thordarson and Larsen 2008), has only 16 entries in the database, and the exceptionally high MI S contents of the Eldgjá 939 eruption warrant more research. There is also a lack of S data from Torfajökull, the largest producer of silicic magmas among active volcanoes in Iceland (Gunnarsson et al. 1998). These would all be desirable targets for further melt inclusion studies.

Sulfur in the deep crust and mantle. The relative effects of melt degree, mantle source heterogeneity and sulfide saturation on S systematics in Iceland remain largely unexplored. Filling this fundamental knowledge gap should provide a fruitful topic for future studies.

Volatile budgets of silicic eruptions. It is likely that silicic magmas in Iceland develop MVPs that provide significant sources of excess degassing not included in the petrological method presented here. However, as no silicic eruptions have occurred during recent history in Iceland, S degassing (and that of other volatiles) accompanying silicic volcanism in Iceland remains poorly constrained. An important task for future research should be to better understand both volcanic S and halogen pollution hazards of silicic eruptions in Iceland.

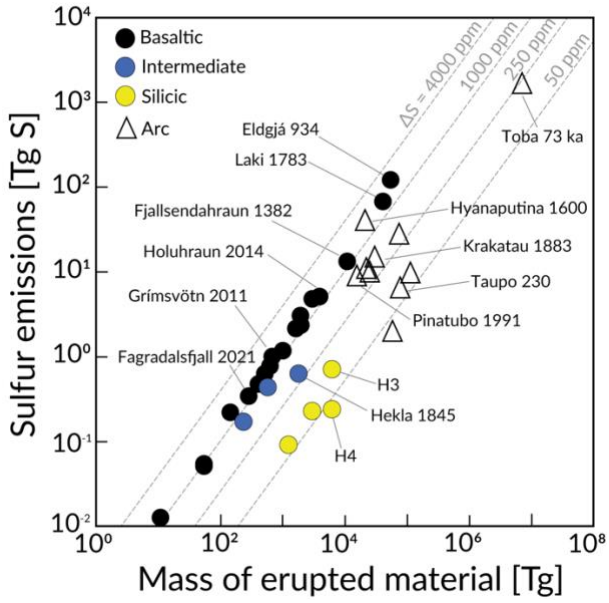

Figure 10. Sulfur emissions of Icelandic eruptions based on the petrological method. Notable arc eruptions are shown for comparison (Oppenheimer et al. 2011 and references therein).

Table 1: Inventory

Reference	Volcano[1]	Eruptions	Mafic	Interm.	Silicic	MI	MG	H_2O	CO_2	F	Cl	S	B	Methods
Sigurdsson1982	Grí	Laki1783				x	x					x		EPMA
Devine1984	Grí, He, Kat, Kra, Ve	Multiple	x		x	x	x					x		EPMA
Óskarsson1984	Grí	Laki1783	x			x	x					x		
Palais1989	Kat, Ör	Eldgjá, 1362 (Ör.)	x		x							x		EPMA
Métrich1991	Grí	Laki1783	x			x	x					x		EPMA
Þórðarson1996	Grí	Laki1783				x	x			x	x	x		EPMA
Þórðarson2001	Kat	Eldgjá	x			x	x					x		EPMA
Þórðarson2003	Bár	Þjórsárhraun										x		EPMA
Moune2007	Hek	1913, 2000	x	x		x	x	x		x	x	x		EPMA, SIMS
Sharma2008	Ör	1362			x	x	x			x	x	x		EPMA
Portnyagin2012	Hek	H3, H4		x	x	x	x	x		x	x	x	x	EPMA, SIMS, FTIR
Owen2012	Tor	Multiple			x	x	x	x			x			SIMS, FTIR
Moune2012	Eyj	Fimmvörðuháls2010	x			x		x		x	x	x		EPMA, SIMS
Brounce2012	Grí	Laki1783	x					x	x	x	x	x	x	SIMS
Sigmarsson2013	Grí	Grímsvötn2011	x			x	x					x		EPMA
Hartley2014	Grí	Laki1783	x			x	x	x	x					EPMA, SIMS, Raman
Neave2014	ERZ	Skuggafjöll	x			x		x	x	x		x		EPMA, SIMS, Raman
Schattel2014	Ask, Ör	1875 (Ask.), 1362 (Ör.)			x	x	x	x		x	x	x		EPMA, SIMS, FTIR
Schipper2016	Ves	Surtsey1963-7	x			x	x	x	x	x	x	x		SIMS
Gauthier2016	Bár	Holuhraun2014-15	x			x	x			x	x	x		EPMA
Lucic2016	Hek	H3, 1104, 1845, 1991		x	x	x	x	x	x		x	x		EPMA, FTIR
Haddadi2017	Grí	G1823, 1873, 2004, 2011	x			x	x	1	1	x	x	x		EPMA
Neave2017	Grí	Saksunarvatn	x			x	x	x	x	x	x	x	x	EPMA, SIMS
Hauri2018	The	Borgarhraun	x			x		x	x	x	x	x		SIMS
Hartley2018	Bár	Holuhraun2014-15											x	SIMS/EPMA
Bali2018	Bár	Holuhraun2014-15	x			x	x	x	x	x	x	x		EPMA, SIMS, FTIR, Raman
Liu2018	Kra	Hverfjall	x			x	x	x	x		x	x		FTIR, EPMA
Miller2019	WRZ	Miðfell	x			x	x	x	x	x	x	x		EPMA, SIMS
Caracciolo2020	Bár	Multiple	x			x	x				x	x		EPMA, SIMS
Hartley2021	Ask	Multiple	x		x	x	x	x	x	x	x	x	x	EPMA, SIMS, Raman
Matthews2021	Rey, Ljó, Fre	Multiple	x			x	x		x	x	x	x	x	EPMA, SIMS
Rooyakkers2021	Kra	Multiple			x	x	x				x	x		EPMA
Ranta2022	Kve	Multiple	x			x	x	x	x		x	x		EPMA, FTIR
Caracciolo2022	Bár	Multiple	x			x	x				x	x		EPMA
Marshall2022	Bár	Holuhraun2014-15	x			x	x						x	SIMS
Halldórsson2022	Fag	Fagradalsfjall2021	x			x	x	x	x		x	x		SIMS, EPMA
This study	Ves, Snæ, Ljó, Bár, Ör	Multiple	x	x		x	x				x	x		EPMA

[1]Ask = Askja; Bár = Bárðarbunga; Bre = Brennisteinsfjöll; ERZ = Eastern Rift Zone (subglacial); Fag = Fagradalsfjall; Fre = Fremrinámar; Grí = Grímsvötn; Hei = Heimaey; Hek = Hekla; Kat = Katla; Kra = Krafla; Krý = Krýsuvík; Kve = Kverkfjöll; Ljó = Ljósufjöll; Rey = Reykjanes; Snæ = Snæfellsjökull; Sv = Svartsengi; Tor = Torfajökull; Þey = Þeystareykir; Sur = Surtsey; WRZ = Western Rift Zone (subglacial); Ör = Öræfajökull.

Table 2: Sulfur emission potentials

Eruption	Volcano	Zone	Composition	ΔS_{vent}	ΔS_{max}[b]	SiO_2[a]	MgO	Na_2O+K_2O
Holuhraun (old)	Bar	ERZ	Basaltic	1077	1077	49.6	6.5	2.6
Veiðivötn 1477	Bar	ERZ	Basaltic	1103	1332	49.6	6.4	2.6
Ljósufjöll	Bar	ERZ	Basaltic	1079	1271	49.4	8.2	1.9
Þjórsárdalshraun	Bar	ERZ	Basaltic	1216	1476	48.9	6.5	2.5
Fontur[c]	Bar	ERZ	Basaltic	513	1306	49.7	6.2	2.6
Brandur[c]	Bar	ERZ	Basaltic	410	1183	50.1	6.7	2.4
Saxi[c]	Bar	ERZ	Basaltic	910	1408	49.6	6.3	2.4
Holuhraun 2014-15	Bar	ERZ	Basaltic	1311	1644	49.8	6.8	2.5
Fjallsendahraun 1382	Bar	ERZ	Basaltic	1225	1587	49.7	6.8	2.7
Þjórsárhraun	Bar	ERZ	Basaltic		1661			
2004	Gri	ERZ	Basaltic	1006	1677	50.5	4.8	3.4
Laki1783	Gri	ERZ	Basaltic	1662	1759	49.4	5.2	3.3
1823	Gri	ERZ	Basaltic	1253	1660	50.7	5.5	3.2
1873	Gri	ERZ	Basaltic	1789	1789	50.6	5.2	3.3
2011	Gri	ERZ	Basaltic	1480	1982	49.8	5.1	3.2
Saksunarvatn	Gri	ERZ	Basaltic	976	1725	49.5	5.4	3.1
Skuggafjöll	ERZ	ERZ	Basaltic		681			
1875	Ask	NRZ	Silicic	-161	200	72.3	0.7	6.4
NE tuff	Ask	NRZ	Basaltic	902	902	49.8	7.1	2.5
SW tuff	Ask	NRZ	Basaltic	1122	1122	50.7	6.8	2.7
Nyjahraun	Ask	NRZ	Basaltic	1468	1468	52.1	4.2	1.9
Heilagsdalsfjall	Fre	NRZ	Basaltic	501	673	48.6	9.1	1.7
Gæsarfjallarani	Kra	NRZ	Silicic		69			
Hlíðarfjall	Kra	NRZ	Silicic	53	53		75.7	0.1
Jörundur	Kra	NRZ	Silicic	63	63		74.9	0.1
Víti	Kra	NRZ	Silicic	14	48		75.7	0.1
Hverfjall	Kra	NRZ	Basaltic	1528	1737	50.7	5.7	2.6
1981	Kra	NRZ	Basaltic	612	738	49.2	6.8	2.4
Subglacial	Kve	NRZ	Basaltic		1649	50.7	4.0	3.4
Borgarhraun	The	NRZ	Basaltic		1077			
1362	Ör	ÖVZ	Silicic	77	240	71.5	0.0	8.6
Fagradalsfjall 2021	Fag	RP	Basaltic	1171	1171	50.0	7.8	2.2
Húsfellsbrúni	Bre	RP	Basaltic	1392	1485	48.9	7.0	2.3
Hvammahraun	Bre	RP	Basaltic	1684	1850	49.0	7.5	2.1
Kistuhraun	Bre	RP	Basaltic	1321	1467	48.8	7.2	2.2
mid-Húsfellsbrúni	Bre	RP	Basaltic	1537	1740	49.0	7.2	2.2
Selvogshraun	Bre	RP	Basaltic	1225	1405	48.4	7.5	2.2
Svartihryggur	Bre	RP	Basaltic	987	1319	48.9	6.7	2.3
Svínahraunsbrúni	Bre	RP	Basaltic	1393	1563	48.7	6.9	2.2
Tvíbollahraun	Bre	RP	Basaltic	1173	1357	48.7	7.6	2.0
Hrútafellshraun	Kry	RP	Basaltic	1241	1546	49.5	6.9	2.2
Kapelluhraun	Kry	RP	Basaltic	1173	1394	49.6	7.0	2.4
Mávahlídarhraun	Kry	RP	Basaltic	947	1288	49.1	7.0	2.5
Ögmundarhraun	Kry	RP	Basaltic	1246	1482	49.5	6.9	2.3
Stapafell	Rey	RP	Basaltic	849	1122	49.0	7.7	2.4
Háleyjabunga	Rey	RP	Basaltic		617			
Stampahraun-4	Rey	RP	Basaltic	1171	1495	50.1	6.6	2.3
SÖ-lavas	Sva	RP	Basaltic	1585	1797	49.3	5.8	2.6
Fimmvorduhals 2010	Eya	SIVZ	Basaltic		1890	46.2	4.5	4.0
Eldfell 1973	Hei	SIVZ	Basaltic	514	851	49.1	3.4	6.5
H4	Hek	SIVZ	Silicic	39	42	72.5	0.1	7.6
H3	Hek	SIVZ	Silicic	115	115	68.0	0.5	7.1
1104	Hek	SIVZ	Silicic	74	74	72.5	0.1	7.9
1845	Hek	SIVZ	Intermediate	352	400	60.8	1.2	6.5
1991	Hek	SIVZ	Intermediate	765	765	54.8	2.7	5.5
2000	Hek	SIVZ	Intermediate	731	931	55.2	3.0	4.3
1913	Hek	SIVZ	Basaltic	2630	2630	45.4	4.5	3.2
Eldgjá 939	Kat	SIVZ	Basaltic	2245	2423	46.6	5.3	3.6
1357	Kat	SIVZ	Basaltic	582	1358	46.9	5.0	3.7
Surtsey 1963-7	Sur	SIVZ	Basaltic	1610	2138	47.1	5.9	4.5
Miðfell	WRZ	WRZ	Basaltic	820	1102	47.6	9.7	1.5
Berserkjarhraun	Ljo	SNVZ	Basaltic	1518	1411	48.8	5.8	3.7
Grábrókahraun	Ljo	SNVZ	Basaltic	1093	1129	48.9	6.0	2.4
Ör1	Ör	SNVZ	Basaltic	1348	1499	46.6	5.2	3.7
Ör3	Ör	SNVZ	Basaltic	1238	1734	49.3	5.4	3.0
Djúpalónsvík	Snæ	SNVZ	Basaltic	526	746	51.5	4.3	4.9

[a] SiO_2, MgO, Na_2O+K_2O average value of matrix glass data.

[b] Mean MI S concentration, instead of maximum, used for calculating ΔS_{vent} and ΔS_{max} for silicic and intermediate eruptions

[c] Likely source craters of the ~8.6 ka Þjórsárhraun lava (Caracciolo et al. 2020)

Data references for each eruption are shown in the electronic version of Table 2.

Appendix

Supplementary figures (Figs. S1 and S2) shown after references.

Electronic supplementary tables:

Table S1: Iceland melt inclusion catalogue (IMIC)
Table S2: Summary of volatile emission potentials
Table S3: EPMA data: Matrix glasses
Table S4: EPMA data: Melt inclusions
Table S5: EPMA data: Plagioclase
Table S6: EPMA data: Olivine and clinopyroxene
Table S7: EPMA data: Standards

References

Anderson, A. T. (1974). Chlorine, sulfur, and water in magmas and oceans. *Geological Society of America Bulletin*, 85(9), 1485-1492.

Andres, R. J., Rose, W. I., Kyle, P. R., DeSilva, S., Francis, P., & Gardeweg, M. (1991). Excessive sulfur dioxide emissions from Chilean volcanoes. *Journal of Volcanology and Geothermal Research*, 46(3-4), 323-329.

Bali, E., Hartley, M. E., Halldórsson, S. A., Gudfinnsson, G. H., & Jakobsson, S. (2018). Melt inclusion constraints on volatile systematics and degassing history of the 2014–2015 Holuhraun eruption, Iceland. *Contributions to Mineralogy and Petrology*, *173*(2), 1-21.

Barsotti, S. (2020). Probabilistic hazard maps for operational use: the case of SO2 air pollution during the Holuhraun eruption (Bárðarbunga, Iceland) in 2014–2015. *Bulletin of Volcanology*, 82(7), 1-15.

Barsotti, S., Oddsson, B., Gudmundsson, M. T., Pfeffer, M. A., Parks, M. M., Ófeigsson, B. G., et al. (2020). Operational response and hazards assessment during the 2014–2015 volcanic crisis at Bárðarbunga volcano and associated eruption at Holuhraun, Iceland. *Journal of Volcanology and Geothermal Research*, 390, 106753.

Barth, A., & Plank, T. (2021). The Ins and Outs of Water in Olivine-Hosted Melt Inclusions: Hygrometer vs. Speedometer. *Frontiers in Earth Science*, 9, 343.

Brounce, M., Feineman, M., LaFemina, P., & Gurenko, A. (2012). Insights into crustal assimilation by Icelandic basalts from boron isotopes in melt inclusions from the 1783–1784 Lakagígar eruption. *Geochimica et Cosmochimica Acta*, 94, 164-180.

Caracciolo, A., Bali, E., Guðfinnsson, G. H., Kahl, M., Halldórsson, S. A., Hartley, M. E., & Gunnarsson, H. (2020). Temporal evolution of magma and crystal mush storage conditions in the Bárðarbunga-Veiðivötn volcanic system, Iceland. *Lithos*, *352*, 105234.

Caracciolo, A., Halldórsson, S. A., Bali, E., Marshall, E. W., Jeon, H., Whitehouse, M. J., et al. (2022). Oxygen isotope evidence for progressively assimilating trans-crustal magma plumbing systems in Iceland. *Geology*, *50(7), 796-800.*

Carlsen, H. K., Ilyinskaya, E., Baxter, P. J., Schmidt, A., Thorsteinsson, T., Pfeffer, M.A., et al. (2021). Increased respiratory morbidity associated with exposure to a mature volcanic plume from a large Icelandic fissure eruption. *Nature communications*, 12(1), 1-12.

Carn, S. A., Fioletov, V. E., McLinden, C. A., Li, C., & Krotkov, N. A. (2017). A decade of global volcanic SO2 emissions measured from space. *Scientific reports*, *7*(1), 44095.

Danyushevsky, L. V., Della-Pasqua, F. N., & Sokolov, S. (2000). Re-equilibration of melt inclusions trapped by magnesian olivine phenocrysts from subduction-related magmas: petrological implications. *Contributions to Mineralogy and Petrology*, 138, 68-83.

Devine, J. D., Sigurdsson, H., Davis, A. N., & Self, S. (1984). Estimates of sulfur and chlorine yield to the atmosphere from volcanic eruptions and potential climatic effects. *Journal of Geophysical Research: Solid Earth*, *89*(B7), 6309-6325.

Ding, S., & Dasgupta, R. (2018). Sulfur inventory of ocean island basalt source regions constrained by modeling the fate of sulfide during decompression melting of a heterogeneous mantle. *Journal of Petrology*, *59*(7), 1281-1308.

Edmonds, M., & Woods, A. W. (2018). Exsolved volatiles in magma reservoirs. *Journal of Volcanology and Geothermal Research*, 368, 13-30.

Füri, E., Hilton, D. R., Halldórsson, S. A., Barry, P. H., Hahm, D., Fischer, T. P., & Grönvold, K. (2010). Apparent decoupling of the He and Ne isotope systematics of the Icelandic mantle: The role of He depletion, melt mixing, degassing fractionation and air interaction. *Geochimica et cosmochimica acta*, 74(11), 3307-3332.

Furman, T., Frey, F. A., & Park, K. H. (1991). Chemical constraints on the petrogenesis of mildly alkaline lavas from Vestmannaeyjar, Iceland: the Eldfell (1973) and Surtsey (1963–1967) eruptions. *Contributions to Mineralogy and Petrology*, 109(1), 19-37.

Gaetani, G. A., O'Leary, J. A., Shimizu, N., Bucholz, C. E., & Newville, M. (2012). Rapid reequilibration of H2O and oxygen fugacity in olivine-hosted melt inclusions. *Geology*, 40(10), 915-918.

Gaillard, F., Bouhifd, M. A., Füri, E., Malavergne, V., Marrocchi, Y., Noack, L., et al. (2021). The diverse planetary ingassing/outgassing paths produced over billions of years of magmatic activity. *Space Science Reviews*, *217*, 1-54.

Gauthier, P. J., Sigmarsson, O., Gouhier, M., Haddadi, B., & Moune, S. (2016). Elevated gas flux and trace metal degassing from the 2014–2015 fissure eruption at the Bárðarbunga volcanic system, Iceland. *Journal of Geophysical Research: Solid Earth*, 121(3), 1610-1630.

Gíslason, S. R., Stefansdottir, G., Pfeffer, M., Barsotti, S., Jóhannsson, T., Galeczka, I. M., et al. (2015).

Environmental pressure from the 2014–15 eruption of Bárðarbunga volcano, Iceland. *Geochemical Perspectives Letters*, 1(0), 84-93

Gunnarsson, B., Marsh, B.D., Taylor Jr., H.P. (1998) Generation of Icelandic rhyolites: silicic lavas from the Torfajökull central volcano. *Journal of Volcanology and Geothermal Research* 83, 1–45.

Haddadi, B., Sigmarsson, O., & Larsen, G. (2017). Magma storage beneath Grímsvötn volcano, Iceland, constrained by clinopyroxene-melt thermobarometry and volatiles in melt inclusions and groundmass glass. *Journal of Geophysical Research: Solid Earth*, *122*(9), 6984-6997.

Halldórsson, S. A., Barnes, J. D., Stefánsson, A., Hilton, D. R., Hauri, E. H., & Marshall, E. W. (2016a). Subducted lithosphere controls halogen enrichments in the Iceland mantle plume source. *Geology*, 44(8), 679-682.

Halldórsson, S. A., Hilton, D. R., Barry, P. H., Füri, E., & Grönvold, K. (2016b). Recycling of crustal material by the Iceland mantle plume: new evidence from nitrogen elemental and isotope systematics of subglacial basalts. *Geochimica et Cosmochimica Acta*, 176, 206-226.

Halldórsson, S. A., Marshall, E. W., Caracciolo, A., Matthews, S., Bali, E., Rasmussen, M. B., et al. (2022). Rapid shifting of a deep magmatic source at Fagradalsfjall volcano, Iceland. *Nature*, *609*(7927), 529-534.

Harðardóttir, S., Halldórsson, S. A., & Hilton, D. R. (2018). Spatial distribution of helium isotopes in Icelandic geothermal fluids and volcanic materials with implications for location, upwelling and evolution of the Icelandic mantle plume. *Chemical Geology*, 480, 12-27.

Harðardóttir, S., Matthews, S., Halldórsson, S. A., & Jackson, M. G. (2022). Spatial distribution and geochemical characterization of Icelandic mantle end-members: Implications for plume geometry and melting processes. *Chemical Geology*, 120930.

Hartley, M. E., Maclennan, J., Edmonds, M., & Thordarson, T. (2014). Reconstructing the deep CO2 degassing behaviour of large basaltic fissure eruptions. *Earth and Planetary Science Letters*, 393, 120-131.

Hartley, M. E., Bali, E., Maclennan, J., Neave, D. A., & Halldórsson, S. A. (2018). Melt inclusion constraints on petrogenesis of the 2014–2015 Holuhraun eruption, Iceland. *Contributions to Mineralogy and Petrology*, *173*(2), 1-23.

Hartley, M. E., De Hoog, J. C., & Shorttle, O. (2021). Boron isotopic signatures of melt inclusions from North Iceland reveal recycled material in the Icelandic mantle source. *Geochimica et Cosmochimica Acta*, *294*, 273-294.

Hauri, E. H., Maclennan, J., McKenzie, D., Gronvold, K., Oskarsson, N., & Shimizu, N. (2018). CO_2 content beneath northern Iceland and the variability of mantle carbon. *Geology*, *46*(1), 55-58.

Hilton, D. R., Thirlwall, M. F., Taylor, R. N., Murton, B. J., & Nichols, A. (2000). Controls on magmatic degassing along the Reykjanes Ridge with implications for the helium paradox. *Earth and Planetary Science Letters*, 183(1-2), 43-50.

Ilyinskaya, E., Mobbs, S., Burton, R., Burton, M., Pardini, F., Pfeffer, M. A., et al. (2018). Globally significant CO_2 emissions from Katla, a subglacial volcano in Iceland. *Geophysical Research Letters*, *45*(19), 10-332.

Ilyinskaya, E., Schmidt, A., Mather, T. A., Pope, F. D., Witham, C., Baxter, P., et al. (2017). Understanding the environmental impacts of large fissure eruptions: Aerosol and gas emissions from the 2014–2015 Holuhraun eruption (Iceland). *Earth and Planetary Science Letters*, 472, 309-322.

Jónasson, K. (2007). Silicic volcanism in Iceland: Composition and distribution within the active volcanic zones. *Journal of Geodynamics*, *43*(1), 101-117.

Koornneef, J. M., Stracke, A., Bourdon, B., Meier, M. A., Jochum, K. P., Stoll, B., & Grönvold, K. (2012). Melting of a two-component source beneath Iceland. *Journal of Petrology*, 53(1), 127-157.

Liu, Y., Samaha, N. T., & Baker, D. R. (2007). Sulfur concentration at sulfide saturation (SCSS) in magmatic silicate melts. *Geochimica et Cosmochimica Acta*, 71(7), 1783-1799.

Liu, E. J., Cashman, K. V., Rust, A. C., & Edmonds, M. (2018). Insights into the dynamics of mafic magmatic-hydromagmatic eruptions from volatile degassing behaviour: The Hverfjall Fires, Iceland. *Journal of Volcanology and Geothermal Research*, 358, 228-240.

Lowenstern, J. B., & Thompson, J. F. H. (1995). Applications of silicate-melt inclusions to the study of magmatic volatiles. Magmas, fluids and ore deposits, 23, 71-99.

Lucic, G., Berg, A. S., & Stix, J. (2016). Water-rich and volatile-undersaturated magmas at Hekla volcano, Iceland. *Geochemistry, Geophysics, Geosystems*, 17(8), 3111-3130.

Maclennan, J. (2017). Bubble formation and decrepitation control the CO_2 content of olivine-hosted melt inclusions. *Geochemistry, Geophysics, Geosystems*, 18(2), 597-616.

Marshall, E. W., Ranta, E., Halldórsson, S. A., Caracciolo, A., Bali, E., Jeon, H., et al. (2022). Boron isotope evidence for devolatilized and rehydrated recycled materials in the Icelandic mantle source. *Earth and Planetary Science Letters*, 577, 117229.

Martin, E., & Sigmarsson, O. (2007). Crustal thermal state and origin of silicic magma in Iceland: the case of Torfajökull, Ljósufjöll and Snæfellsjökull volcanoes. *Contributions to Mineralogy and Petrology*, *153*, 593-605.

Matthews, S., Shorttle, O., Maclennan, J., & Rudge, J. F. (2021). The global melt inclusion C/Ba array: Mantle variability, melting process, or degassing?. *Geochimica et Cosmochimica Acta*, *293*, 525-543.

Miller, W. G., Maclennan, J., Shorttle, O., Gaetani, G. A., Le Roux, V., & Klein, F. (2019). Estimating the carbon content of the deep mantle with Icelandic melt

inclusions. *Earth and Planetary Science Letters*, 523, 115699.

Moune, S., Sigmarsson, O., Thordarson, T., & Gauthier, P. J. (2007). Recent volatile evolution in the magmatic system of Hekla volcano, Iceland. *Earth and Planetary Science Letters*, 255(3-4), 373-389.

Moune, S., Sigmarsson, O., Schiano, P., Thordarson, T., & Keiding, J. K. (2012). Melt inclusion constraints on the magma source of Eyjafjallajökull 2010 flank eruption. *Journal of Geophysical Research: Solid Earth*, *117*(B9).

Métrich, N., Sigurdsson, H., Meyer, P. S., & Devine, J. D. (1991). The 1783 Lakagigar eruption in Iceland: geochemistry, CO2 and sulfur degassing. *Contributions to Mineralogy and Petrology*, *107*(4), 435-447.

Momme, P., Óskarsson, N., & Keays, R. R. (2003). Platinum-group elements in the Icelandic rift system: melting processes and mantle sources beneath Iceland. *Chemical Geology*, *196*(1-4), 209-234.

Moore, L. R., Gazel, E., Tuohy, R., Lloyd, A. S., Esposito, R., Steele-MacInnis, M., et al. (2015). Bubbles matter: An assessment of the contribution of vapor bubbles to melt inclusion volatile budgets. *American Mineralogist*, *100*(4), 806-823.

Neave, D. A., Maclennan, J., Hartley, M. E., Edmonds, M., & Thordarson, T. (2014). Crystal storage and transfer in basaltic systems: the Skuggafjöll eruption, Iceland. *Journal of Petrology*, 55(12), 2311-2346.

Neave, D. A., Hartley, M. E., Maclennan, J., Edmonds, M., & Thordarson, T. (2017). Volatile and light lithophile elements in high-anorthite plagioclase-hosted melt inclusions from Iceland. *Geochimica et Cosmochimica Acta*, *205*, 100-118.

Nichols, A. R. L., Carroll, M. R., & Höskuldsson, Á. (2002). Is the Iceland hot spot also wet? Evidence from the water contents of undegassed submarine and subglacial pillow basalts. *Earth and Planetary Science Letters*, 202(1), 77-87.

O'Neill, H. S. C., & Mavrogenes, J. A. (2002). The sulfide capacity and the sulfur content at sulfide saturation of silicate melts at 1400 C and 1 bar. *Journal of Petrology*, *43*(6), 1049-1087.

Oppenheimer, C., Scaillet, B., & Martin, R. S. (2011). Sulfur degassing from volcanoes: source conditions, surveillance, plume chemistry and earth system impacts. *Reviews in Mineralogy and Geochemistry*, 73(1), 363-421.

Óskarsson N, Grönvold K, Larsen G (1984) The haze produced by the Laki eruption. In Einarsson T, Gudbergsson GM, Gunnlaugsson GA, Rafnsson S, Thorarinsson S (eds) Skaftáreldar 1783–1784 :Ritgerdir og Heimildir. Mál og Menning, Reykjavík, pp 67–80

Owen, J., Tuffen, H., & McGarvie, D. W. (2012). Using dissolved H2O in rhyolitic glasses to estimate palaeo-ice thickness during a subglacial eruption at Bláhnúkur (Torfajökull, Iceland). *Bulletin of volcanology*, 74(6), 1355-1378.

Padilla, A. J., Miller, C. F., Carley, T. L., Economos, R. C., Schmitt, A. K., Coble, M. A., et al. (2016). Elucidating the magmatic history of the Austurhorn silicic intrusive complex (southeast Iceland) using zircon elemental and isotopic geochemistry and geochronology. *Contributions to Mineralogy and Petrology* 171, 69.

Palais, J.M., & Sigurdsson, H. (1989). Petrologic evidence of volatile emissions from major historic and pre-historic volcanic eruptions. *Understanding Climate Change, Geophys. Monogr*. Ser, 52, 31-53.

Pedersen, G. B., Belart, J. M., Óskarsson, B. V., Gudmundsson, M. T., Gies, N., Högnadóttir, T., et al. (2022). Volume, effusion rate, and lava transport during the 2021 Fagradalsfjall eruption: Results from near real-time photogrammetric monitoring. *Geophysical Research Letters*, *49*(13), e2021GL097125.

Pedersen, G. B. M., Höskuldsson, A., Dürig, T., Thordarson, T., Jonsdottir, I., Riishuus, M. S., et al. (2017). Lava field evolution and emplacement dynamics of the 2014–2015 basaltic fissure eruption at Holuhraun, Iceland. *Journal of Volcanology and Geothermal Research*, *340*, 155-169.

Pfeffer, M. A., Bergsson, B., Barsotti, S., Stefánsdóttir, G., Galle, B., Arellano, S., et al. (2018). Ground-based measurements of the 2014–2015 Holuhraun volcanic cloud (Iceland). *Geosciences*, 8(1), 29.

Plank, T., Kelley, K. A., Zimmer, M. M., Hauri, E. H., & Wallace, P. J. (2013). Why do mafic arc magmas contain~ 4 wt.% water on average?. *Earth and Planetary Science Letters*, 364, 168-179.

Poreda, R., Schilling, J. G., & Craig, H. (1986). Helium and hydrogen isotopes in ocean-ridge basalts north and south of Iceland. *Earth and Planetary Science Letters*, 78(1), 1-17.

Portnyagin, M., Hoernle, K., Storm, S., Mironov, N., van den Bogaard, C., & Botcharnikov, R. (2012). H_2O-rich melt inclusions in fayalitic olivine from Hekla volcano: Implications for phase relationships in silicic systems and driving forces of explosive volcanism on Iceland. *Earth and Planetary Science Letters*, 357, 337-346.

Ranta, E. (2022). Stable isotopes of volatile elements as a window into the crust and mantle beneath Icelandic volcanoes. PhD thesis, University of Iceland, pp. 201.

Ranta, E., Gunnarsson-Robin, J., Halldórsson, S. A., Ono, S., Izon, G., Jackson, M. G., et al. (2022). Ancient and recycled sulfur sampled by the Iceland mantle plume. *Earth and Planetary Science Letters*, 584, 117452.

Ranta, E. J., Halldórsson, S. A., Barnes, J. D., Jónasson, K., & Stefánsson, A. (2021). Chlorine isotope ratios record magmatic brine assimilation during rhyolite genesis. *Geochemical Perspectives Letters* 16, 35–39.

Rasmussen, D. J., Plank, T. A., Wallace, P. J., Newcombe, M. E., & Lowenstern, J. B. (2020). Vapor-bubble growth in olivine-hosted melt inclusions. *American Mineralogist: Journal of Earth and Planetary Materials*, 105(12), 1898-1919.

Robock, A. (2000). Volcanic eruptions and climate. Reviews of geophysics, 38(2), 191-219. Rooyakkers, S. M., Stix, J., Berlo, K., Petrelli, M., Hampton, R. L., Barker, S. J., & Morgavi, D. (2021). The origin of

rhyolitic magmas at Krafla Central Volcano (Iceland). *Journal of Petrology*, *62*(8), egab064.

Rooyakkers, S. M., Stix, J., Berlo, K., Petrelli, M., Hampton, R. L., Barker, S. J., & Morgavi, D. (2021). The origin of rhyolitic magmas at Krafla Central Volcano (Iceland). *Journal of Petrology*, *62*(8), egab064.

Scaillet, B., & Pichavant, M. (2003). Experimental constraints on volatile abundances in arc magmas and their implications for degassing processes. *Geological Society, London, Special Publications*, *213*(1), 23-52.

Scaillet, B., Luhr, J., & Carroll, M. R. (2003). Petrological and volcanological constraints on volcanic sulfur emissions to the atmosphere. *Geophysical Monograph - American Geophysical Union*, *139*, 11-40.

Schattel, N., Portnyagin, M., Golowin, R., Hoernle, K., & Bindeman, I. (2014). Contrasting conditions of rift and off-rift silicic magma origin on Iceland. *Geophysical Research Letters*, 41(16), 5813-5820.

Schiavi, F., Bolfan-Casanova, N., Buso, R., Laumonier, M., Laporte, D., Medjoubi, K., et al. (2020). Quantifying magmatic volatiles by Raman microtomography of glass inclusion-hosted bubbles. *Geochemical Perspectives Letters*, 16, 17-24.

Schipper, C. I., Le Voyer, M., Moussallam, Y., White, J. D., Thordarson, T., Kimura, J. I., & Chang, Q. (2016). Degassing and magma mixing during the eruption of Surtsey Volcano (Iceland, 1963–1967): the signatures of a dynamic and discrete rift propagation event. *Bulletin of Volcanology*, *78*(4), 1-19.

Schmidt, A., Ostro, B., Carslaw, K. S., Wilson, M., Thordarson, T., Mann, G. W., & Simmons, A. J. (2011). Excess mortality in Europe following a future Laki-style Icelandic eruption. *Proceedings of the National Academy of Sciences*, 108(38), 15710-15715.

Sharma, K., Blake, S., Self, S., & Krueger, A. J. (2004). SO_2 emissions from basaltic eruptions, and the excess sulfur issue. *Geophysical Research Letters*, 31(13).

Sharma, K., Self, S., Blake, S., Thordarson, T., & Larsen, G. (2008). The AD 1362 Öræfajökull eruption, SE Iceland: Physical volcanology and volatile release. *Journal of Volcanology and Geothermal Research*, 178(4), 719-739.

Shimizu, K., Saal, A. E., Myers, C. E., Nagle, A. N., Hauri, E. H., Forsyth, D. W., et al. (2016). Two-component mantle melting-mixing model for the generation of mid-ocean ridge basalts: Implications for the volatile content of the Pacific upper mantle. *Geochimica et Cosmochimica Acta*, 176, 44-80.

Shinohara, H. (2008). Excess degassing from volcanoes and its role on eruptive and intrusive activity. *Reviews of Geophysics*, 46(4).

Sigmarsson, O., Haddadi, B., Carn, S., Moune, S., Gudnason, J., Yang, K., & Clarisse, L. (2013). The sulfur budget of the 2011 Grímsvötn eruption, Iceland. *Geophysical Research Letters*, 40(23), 6095-6100.

Sigmarsson, O., & Halldórsson, S. A. (2015). Delimiting Bárðarbunga and Askja volcanic systems with Sr-and Nd-isotope ratios. *Jökull*, *65*, 17-27.

Sigmarsson, O., Moune, S., & Gauthier, P. J. (2020). Fractional degassing of S, Cl and F from basalt magma in the Bárðarbunga rift zone, Iceland. *Bulletin of Volcanology*, 82(7), 1-8.

Sigurdsson H (1982) Volcanic pollution and climate: the 1783 Laki eruption. *EOS* 63:601–602

Simmons, I. C., Pfeffer, M. A., Calder, E. S., Galle, B., Arellano, S., Coppola, D., & Barsotti, S. (2017). Extended SO_2 outgassing from the 2014–2015 Holuhraun lava flow field, Iceland. *Bulletin of Volcanology*, 79(11), 1-11.

Smythe, D. J., Wood, B. J., & Kiseeva, E. S. (2017). The S content of silicate melts at sulfide saturation: new experiments and a model incorporating the effects of sulfide composition. *American Mineralogist*, 102(4), 795-803.

Stefánsson, A., Stefánsdóttir, G., Keller, N. S., Barsotti, S., Sigurdsson, Á., Thorláksdóttir, S. B., et al. (2017). Major impact of volcanic gases on the chemical composition of precipitation in Iceland during the 2014–2015 Holuhraun eruption. *Journal of Geophysical Research: Atmospheres*, 122(3), 1971-1982.

Stewart, C., Damby, D. E., Horwell, C. J., Elias, T., Ilyinskaya, E., Tomašek, I., et al. (2022). Volcanic air pollution and human health: recent advances and future directions. *Bulletin of Volcanology*, 84(1), 1-25.

Su, Y., Huber, C., Bachmann, O., Zajacz, Z., Wright, H., & Vazquez, J. (2016). The role of crystallization-driven exsolution on the sulfur mass balance in volcanic arc magmas. *Journal of Geophysical Research: Solid Earth*, 121(8), 5624-5640.

Thordarson, T., & Höskuldsson, Á. (2008). Postglacial volcanism in Iceland. *Jökull*, *58*(198), e228.

Thordarson, T., & Larsen, G. (2007). Volcanism in Iceland in historical time: Volcano types, eruption styles and eruptive history. *Journal of Geodynamics*, *43*(1), 118-152.

Thordarson, T., Miller, D. J., Larsen, G., Self, S., & Sigurdsson, H. (2001). New estimates of sulfur degassing and atmospheric mass-loading by the 934 AD Eldgjá eruption, Iceland. *Journal of Volcanology and Geothermal Research*, *108*(1-4), 33-54.

Thordarson, T., Self, S., Miller, D. J., Larsen, G., & Vilmundardóttir, E. G. (2003). Sulphur release from flood lava eruptions in the Veidivötn, Grímsvötn and Katla volcanic systems, Iceland. *Geological Society, London, Special Publications*, *213*(1), 103-121.

Thordarson, T., Self, S., Oskarsson, N., & Hulsebosch, T. (1996). Sulfur, chlorine, and fluorine degassing and atmospheric loading by the 1783–1784 AD Laki (Skaftár Fires) eruption in Iceland. *Bulletin of Volcanology*, *58*, 205-225.

Þórðardóttir, I. (2020). A microprobe study of tephra glasses from the Fjallsendahraun lava, central Iceland (BSc Thesis, University of Iceland).

Wallace, P. J., & Edmonds, M. (2011). The sulfur budget in magmas: evidence from melt inclusions, submarine glasses, and volcanic gas emissions. *Reviews in Mineralogy and Geochemistry*, *73*(1), 215-246.

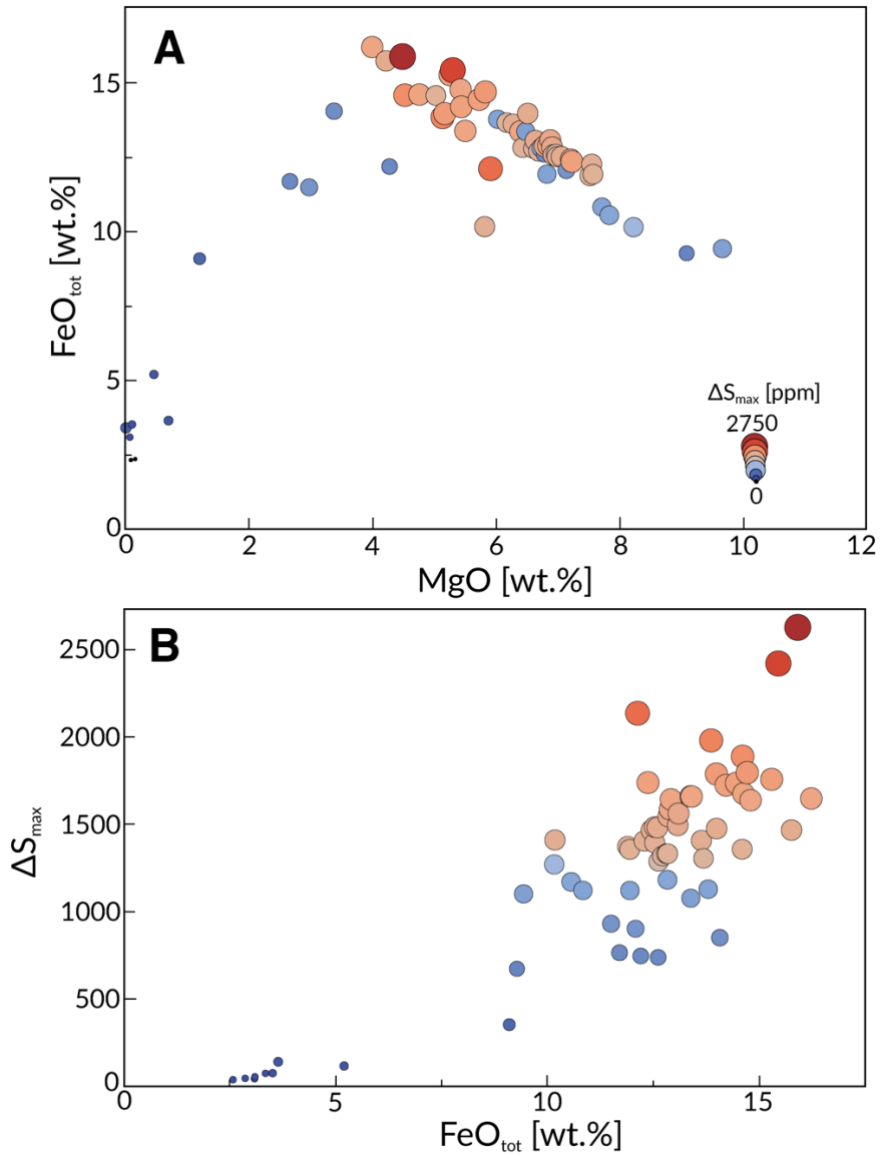

Figure S1 Iron and sulfur. (a) FeO_{tot} vs. MgO. (b) ΔS_{max} vs. FeO_{tot}. FeO content of melts is one of the main controls on sulfur solubility (Smythe et al. 2017), resulting in a broad correlation between ΔS_{max} and FeO_{tot}. However, large variability (> 100%) in ΔS_{max} is observed at a given FeO_{tot}, demonstrating the juxtaposed effects of pressure, temperature and fO_2 on the SCSS, as well as the likely presence of sulfide undersaturated melts at higher MgO. Circles represent individual eruptions and are shaded from blue to red and increase in size with increasing ΔS_{max}.

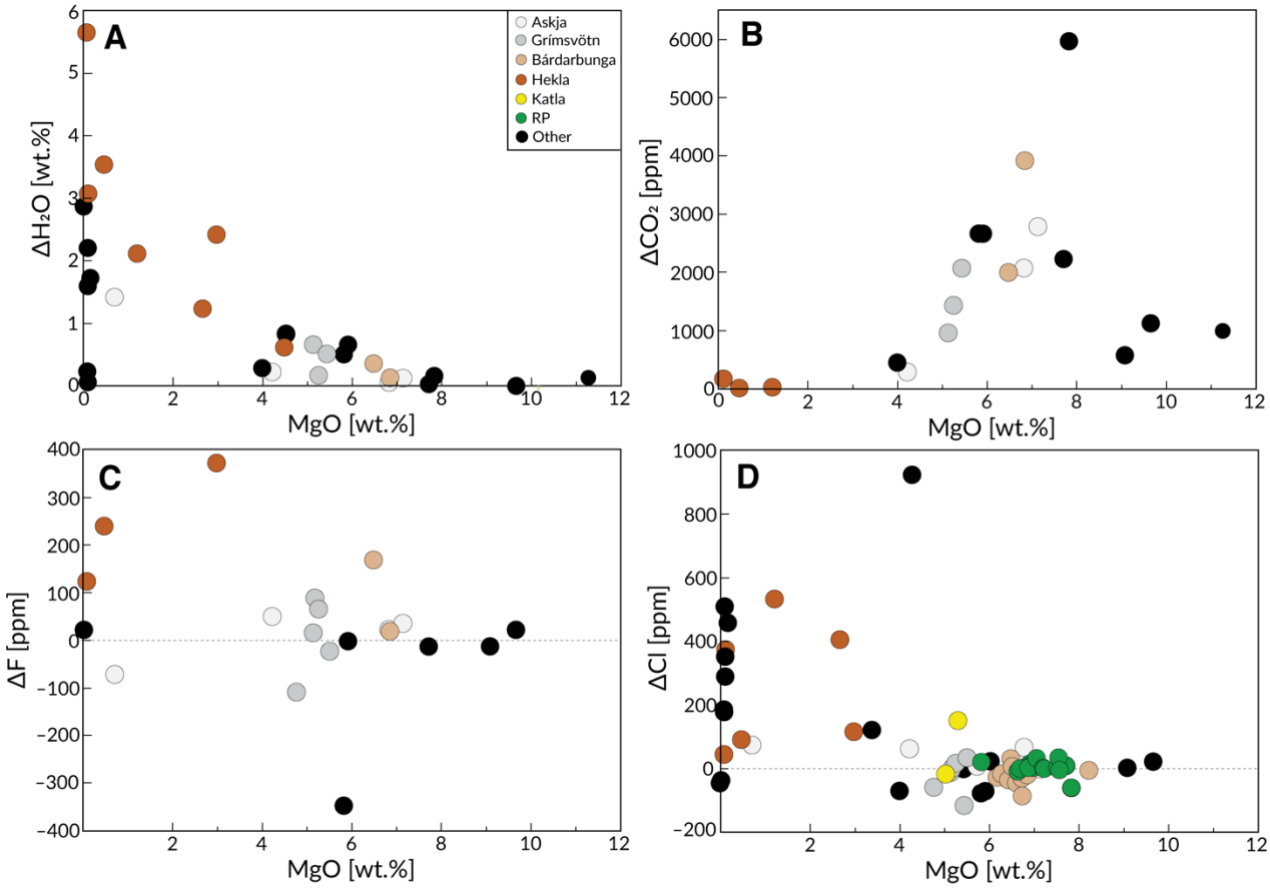

Figure S2: Application of the petrological method for (a) H_2O, (b) CO_2, (c) Cl and (d) F vs. MgO. The volatile emission estimates for these volatiles are not considered to be as accurate as for sulfur (see Section 5).